

# **EFFECTS OF HOT STREAK AND PHANTOM COOLING ON HEAT TRANSFER IN A COOLED TURBINE STAGE INCLUDING PARTICULATE DEPOSITION**

**THE OHIO STATE UNIVERSITY**

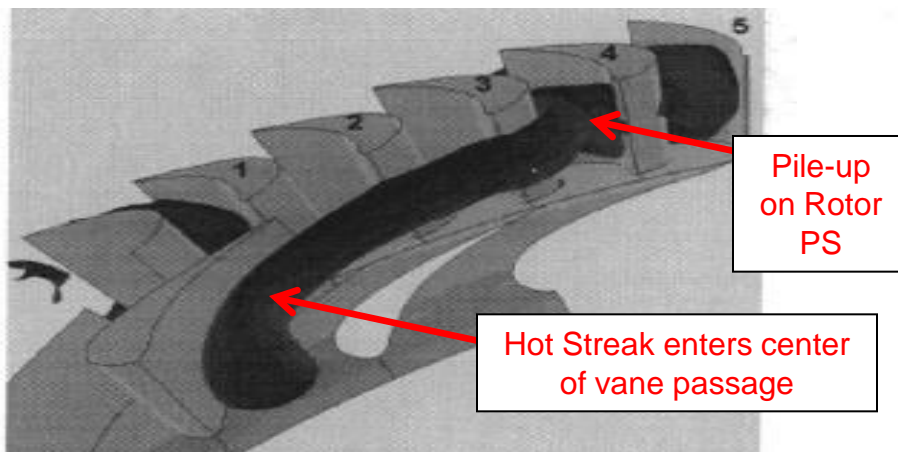
**Brian Casaday, Derek Lageman**

**Ali Ameri, Jeffrey Bons**

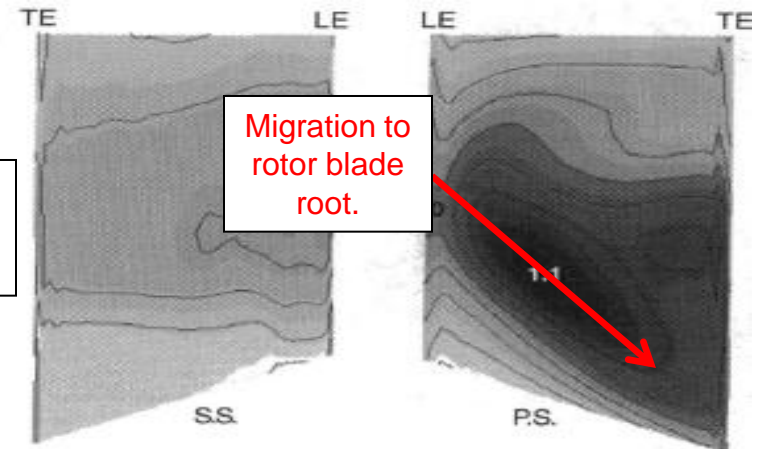
**2011 UTSR Workshop – 26 Oct. 2011**

# MOTIVATION

- Future gas turbines operating with HHC fuels will have higher turbine inlet temperatures relative to natural gas operation.
- Increased temperatures require better materials and more efficient cooling schemes. Increased cooling is unacceptable, so coolant must be used smarter and more sparingly.
- Requires better prediction of combustor exit temperature distribution (pattern factor) and migration of high temperature core (hot streak) through high pressure turbine.



Prediction of hot streak migration in uncooled turbine stage using inviscid, unsteady simulation. (Shang & Epstein, JTurbo 1997)



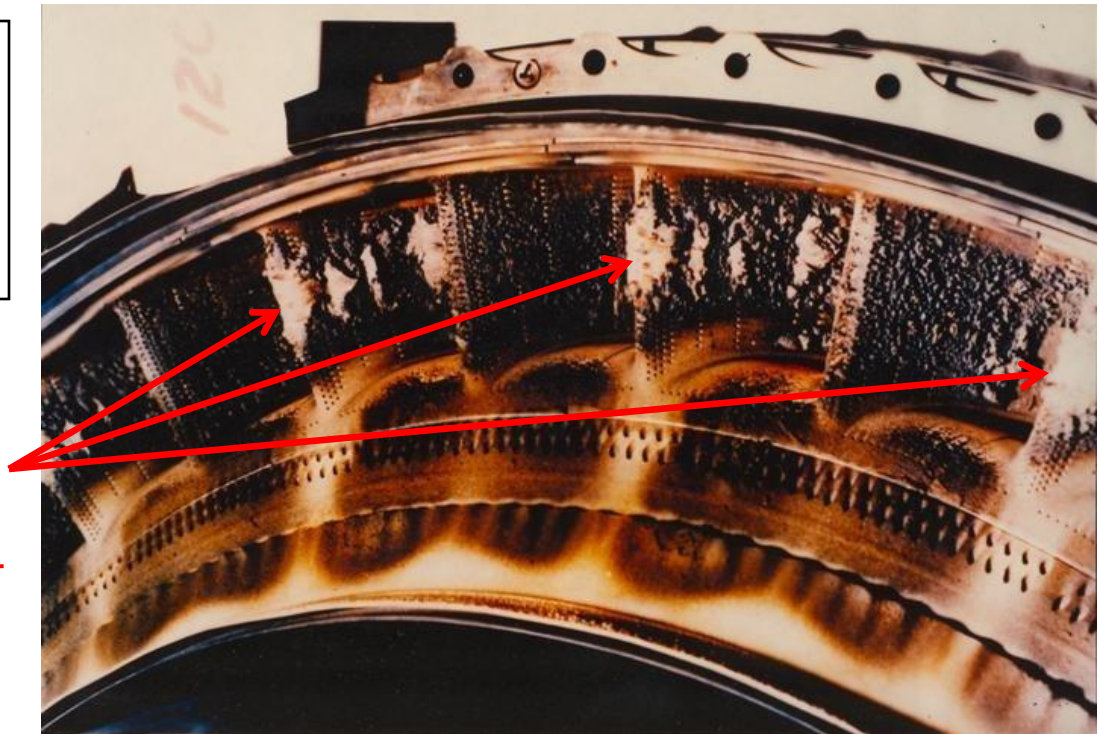
Time averaged surface temperature on rotor suction (left) and pressure (right) surfaces.

# MOTIVATION

- HHC fuels may contain airborne ash particulate that then deposits in the turbine – degrading performance. Hot streaks will result in preferential deposition. Predictive tools for modeling the combined effect of hot streaks and deposition are necessary for risk assessment and mitigation.

First stage nozzle volcanic ash deposition from RB211 following Mt Gallungung eruption, 24 June 1982 (Chambers)

Elevated ash deposition aligned with fuel nozzle locations - evident every other NGV



# CRITICAL NEED

**Additional research is NEEDED to...**

- **model hot streak migration in a modern, cooled first stage turbine**
- **model effect of hot streak on coolant flow (phantom cooling)**
- **model deposition in HHC, elevated temperature environment**
- **validate models with steady (stator) and unsteady (rotor) experimental data**

# OBJECTIVES

- The objective of this work is to develop a validated modeling capability to characterize the effect of hot streaks on the heat load of a modern gas turbine.
- As a secondary objective the model will also be able to predict deposition locations and rates.

This will be accomplished for a cooled turbine stage (stator and rotor)  
AND  
will be validated with experimental data from facilities at OSU.

The effort includes both experimental and computational components, with work divided into three phases of increasing complexity:

- 1) Uncooled Vane
- 2) Cooled Vane
- 3) Uncooled/Cooled Rotor

# RESEARCH TEAM

## **TEAM LEAD**

Focus: Experimental Heat Transfer and Deposition Measurements in OSU Hot Cascade Facility



**Dr. Jeffrey Bons**

Professor  
Department of Mechanical and Aerospace Engineering  
Ohio State University  
Columbus, OH

## **Co-PI**

Focus: Deposition Model Development and Heat Transfer CFD



**Dr. Ali Ameri**

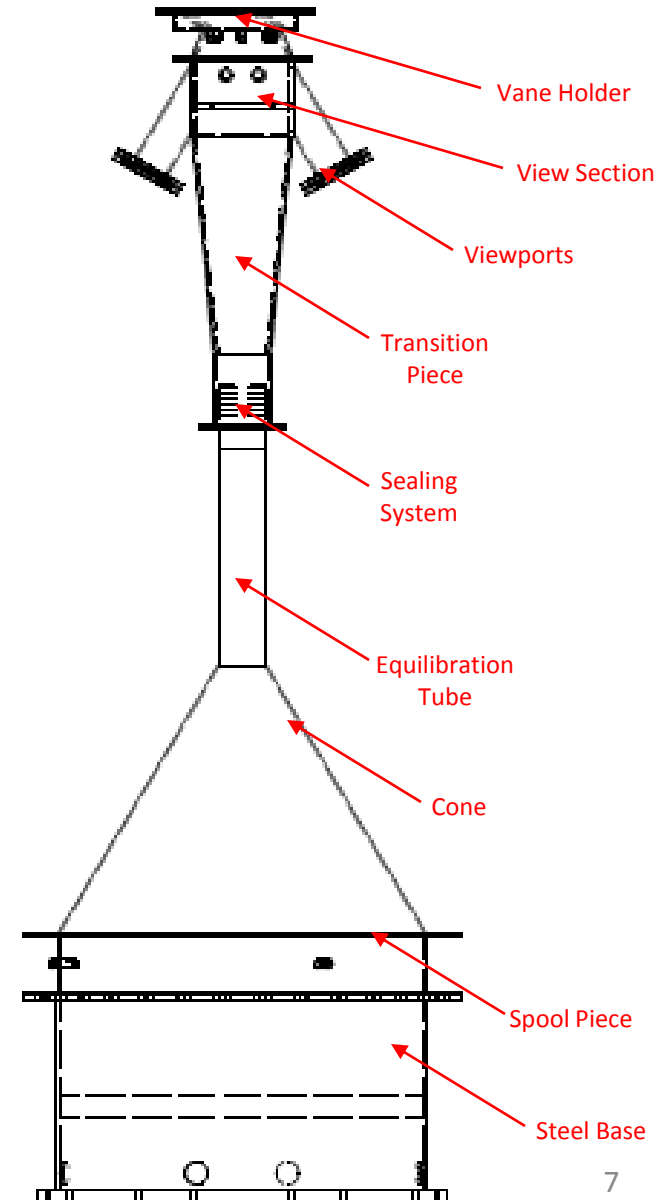
Research Scientist  
Department of Mechanical and Aerospace Engineering  
Ohio State University  
Columbus, OH



# OSU's Turbine Reacting Flow Rig (TuRFR)

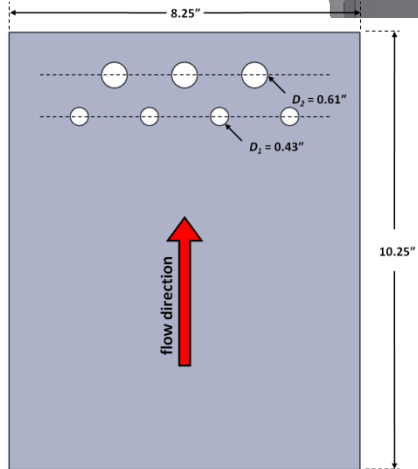
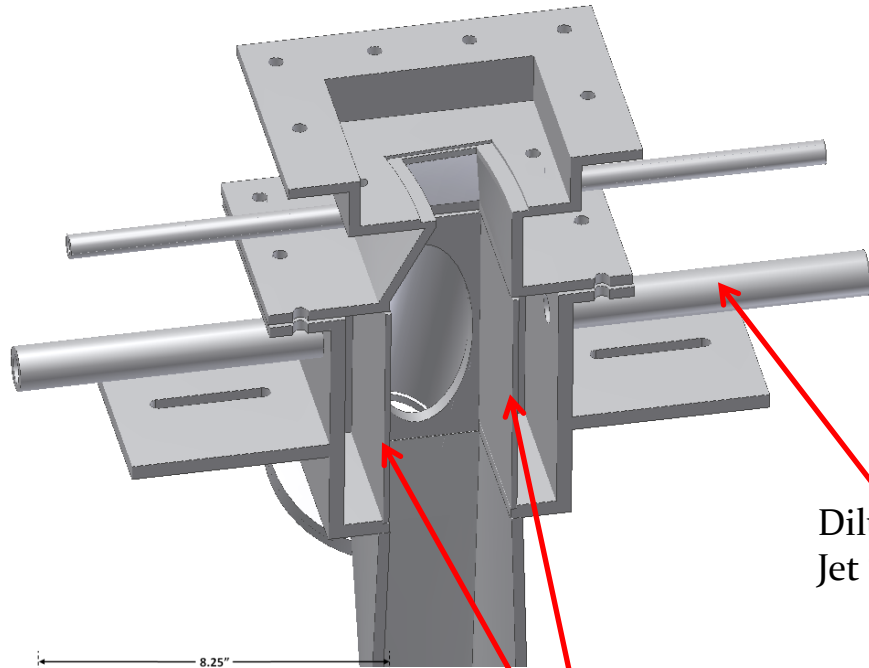


- Natural gas burning combustor rig
- Combustor exit flow accelerated in cone nozzle
- Transition from circular to annular sector
- Real vane hardware (industry supplied) installed in annular cascade sector
- Tt4 up to 1120°C (2050°F)
- Inlet Mach number  $\sim 0.1$
- $300,000 < Re_{cex} < 1,000,000$
- Adjustable inlet temperature profiles
- Adjustable inlet turbulence profiles (through dilution jets)
- Film cooling from vane casing and hub (density ratio 1.6-2.0)
- Ash particulate feed in combustion chamber (10  $\mu\text{m}$  MMD)



# OSU's Turbine Reacting Flow Facility (TuRFR)

## Vane Holder and Upstream Conditioning



Film Cooling Supply

Dilution Jet Supply

Top Section/  
Vane container

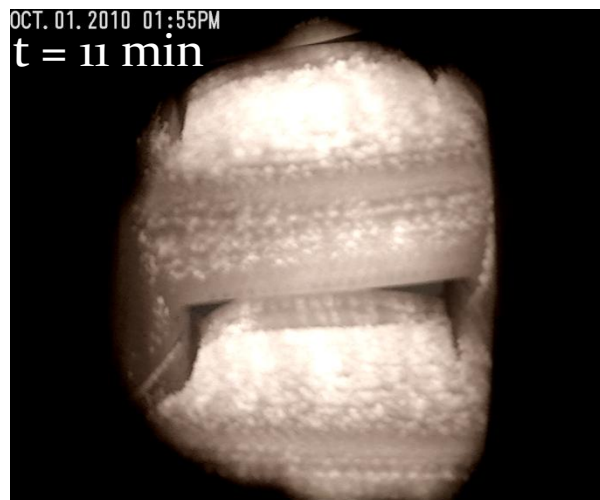
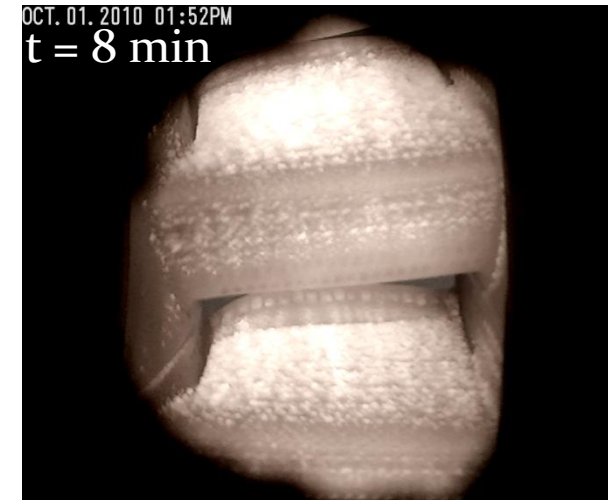
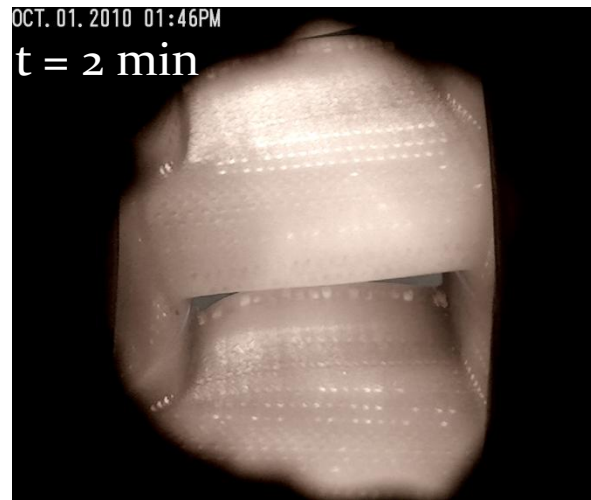
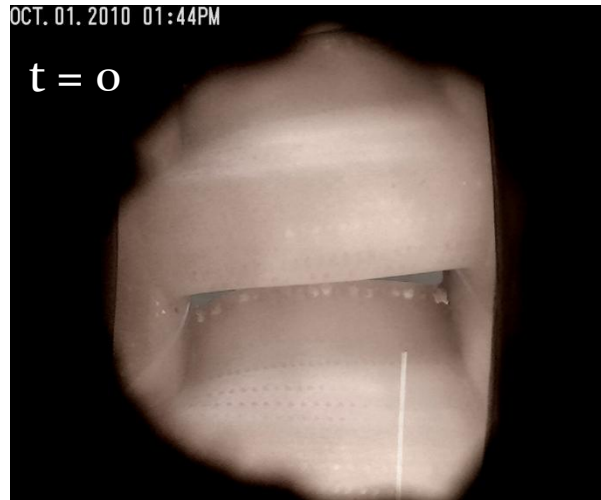
Rectangular to Annular Transition

Circular to Rectangular Transition

Interchangeable Dilution Plates for Pattern Factors

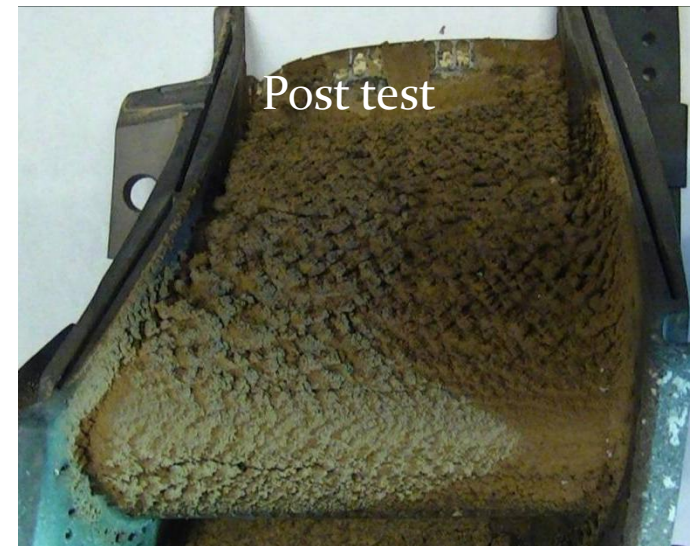


# Typical TuRFR Test Sequence



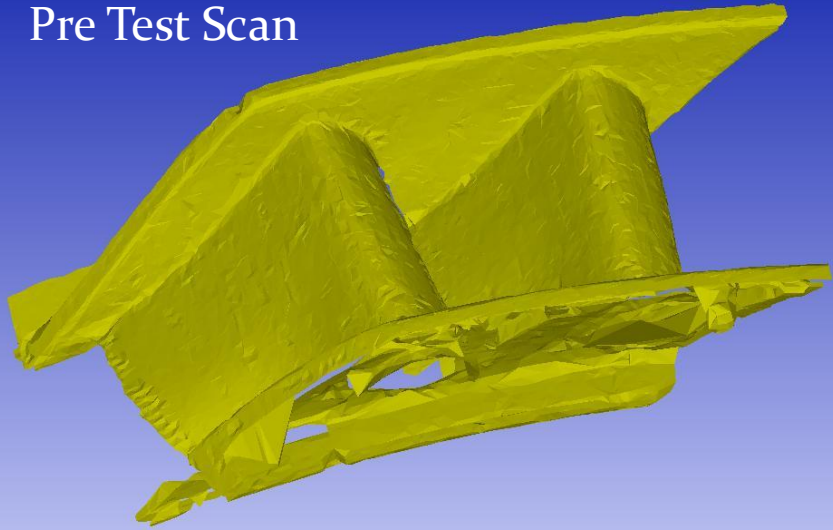
Time Lapse Images  
Wyoming  
Sub-Bituminous Ash  
Test Conditions:

$T_{t4} \sim 1900\text{F}$   
 $M_{in} = 0.90$

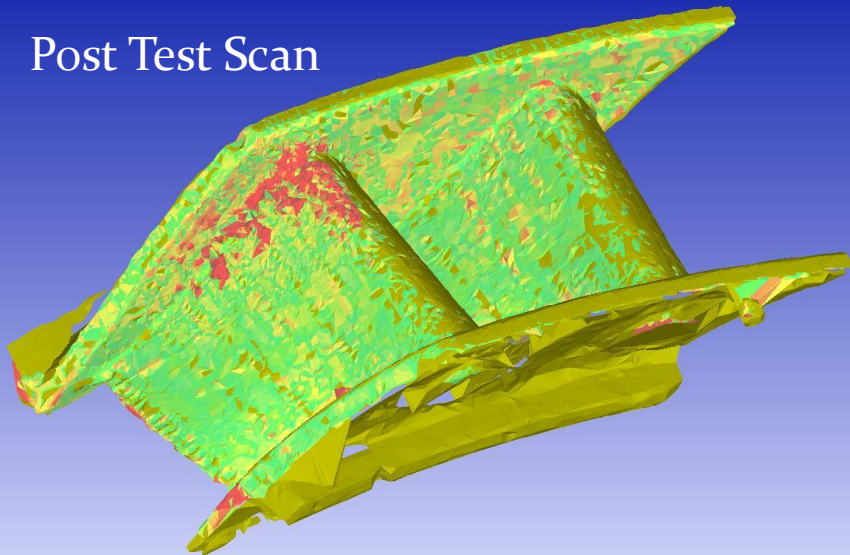


# Post Test Diagnostics - Metrology

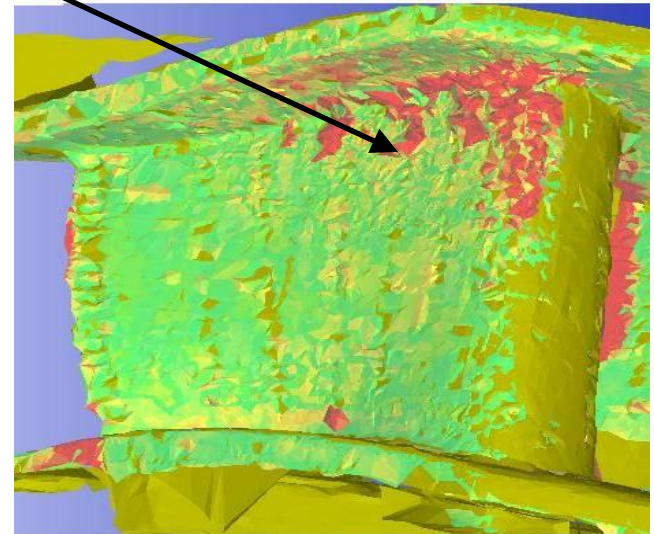
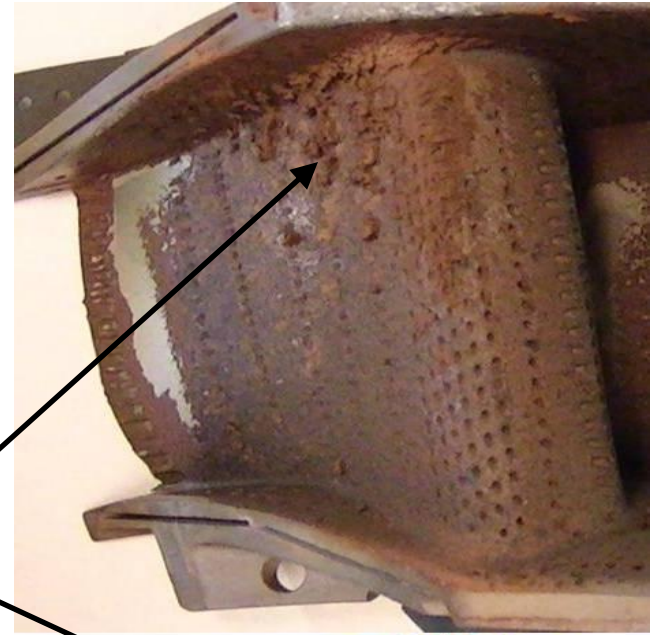
Pre Test Scan



Post Test Scan



Deposit height  
indicated in  
contour map  
relative to Pre-  
Test Datum



# PHASE 1: Uncooled Vane

- Revisit OSU's current deposition model
- Consult with industry to determine representative hot streak for power turbine.
- Generate hot streak in TuRFR
- Measure hot streak migration and adiabatic wall temperature (uncooled vane)
- Measure deposition patterns and rates with hot streaks
- Compare model predictions with TuRFR hot streak and deposition measurements.
- Modify model as needed.

# PHASE 2: Cooled Vane

- Measure hot streak migration and wall temperature for cooled vane
- Measure deposition patterns and rates with hot streaks for cooled vane
- Compare model predictions with TuRFR hot streak and deposition measurements.
- Modify model as needed.
- Propose and explore design modifications that will mitigate particulate deposition on turbine vanes.

# PHASE 3: Rotor

- Incorporate deposition model into unsteady rotor-stator code
- Extract hot streak data from OSU GTL rotating uncooled turbine test data
- Extract hot streak data from OSU GTL rotating cooled turbine test data
- Geometry modeling and gridding
- Compare model predictions with rotating data.
- Modify model as needed.
- Propose and explore design modifications that will mitigate particulate deposition on turbine rotors.



# Accomplishments

- Fabricated dilution plates for hot streak generation in TuRFR
- Preliminary CFD Study:
  - model hot streak migration in E<sup>3</sup> vane.
  - model deposition with hot streak in E<sup>3</sup> vane using critical viscosity deposition model.
- Canvassing literature for improved deposition models
- Actively pursuing sources for unsteady hot streak data



# Preliminary Hot Streak CFD Study

- Modeling Background
  - Particle Trajectory
  - Deposition Models
  - Verification
- Hot Streak Modeling
  - Model Specifications
  - Modeling Results
- Further Work
- Data

# Background

Numerical study of deposition growth on 3D turbine vanes by:

- Accurate capturing of flow physics for 3D turbine passage
- Utilizing models for predicting particle trajectories in 3D flow fields
- Utilizing existing deposition models while exploring mechanisms for improved modeling
- Locating areas of high deposition and determining causes of increased deposition

# Trajectory

## Eulerian-Lagrangian Approach

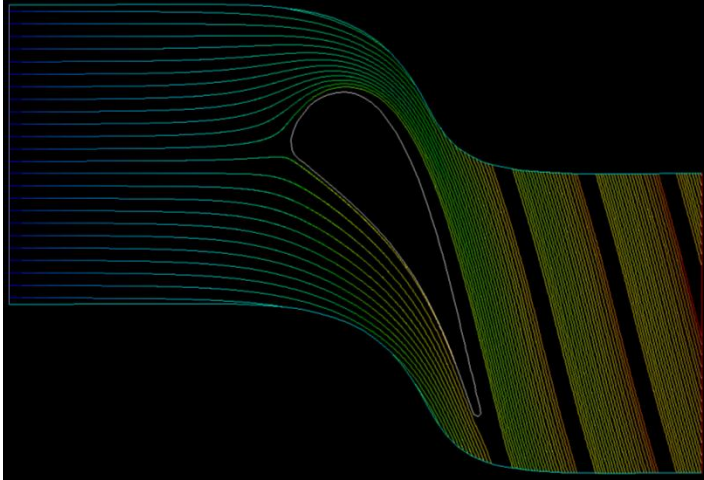
### Particle Trajectories were modeled in FLUENT

- Eulerian-Lagrangian Model
  - Flow solution obtained first using Eulerian approach
  - Particles (dispersed phase) tracked using Lagrangian Model
- Assumptions
  - Particle loading is very low  $\frac{\dot{m}_{\text{Particulate}}}{\dot{m}_{\text{Air}}} < 10^{-6}$
  - Particle-particle interactions are neglected
  - Turbulence and flow modifications due to particles are insignificant and are therefore neglected

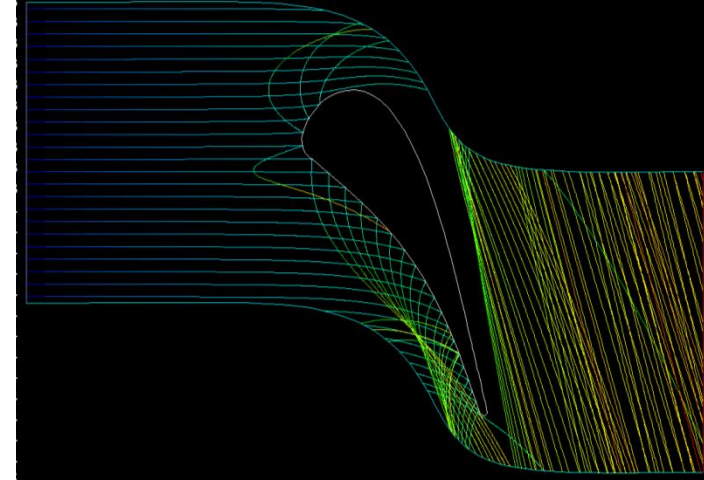
## Dispersed Phase

- Lagrangian approach solves the dispersed phase by integrating the particle equation of motion.
- **Forces considered:** drag force modified with Cunningham correction factor, Saffman Lift Force
- **Forces not considered:** Thermophoretic, Brownian, Magnus, History effect, Gravitational, Buoyancy, Intercollision

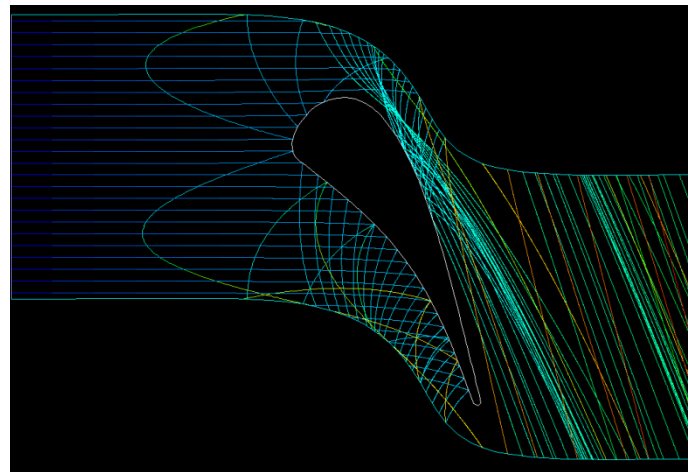
# Trajectory



1 μm particles  
( $St_k = 0.01$ )



20 μm particles  
( $St_k = 4.0$ )



50 μm particles  
( $St_k = 25$ )

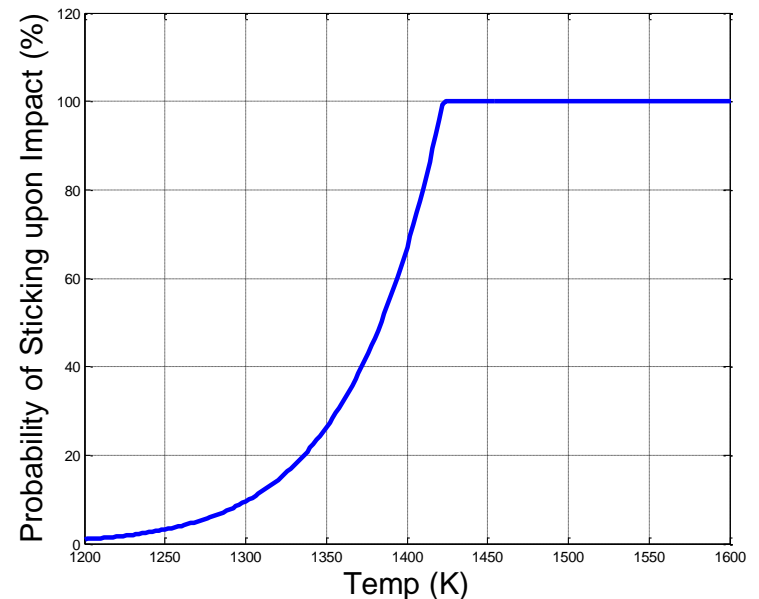
# Deposition Models

- We use two models for deposition
- **Critical Velocity** and **Critical Viscosity**
- The Crit. Vis. model, for many known compositions, may be used without the need for empirical fitting.

$$P_S(T_p) = \frac{\mu_{crit}}{\mu_{T_p}}$$

$$\log\left(\frac{\mu}{T_p}\right) = A + \frac{10^3 B}{T_p}$$

- Viscosity-Temperature relationship (Senior et al.) is used.

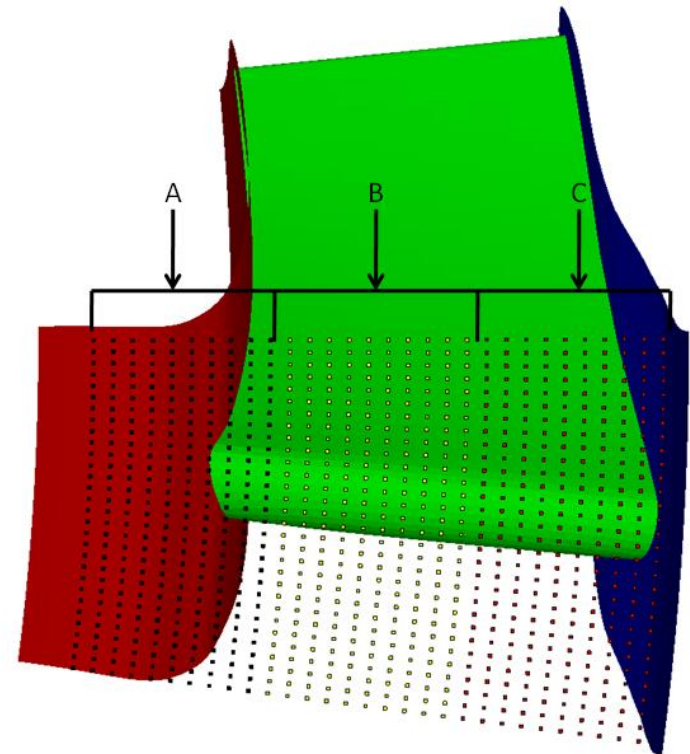




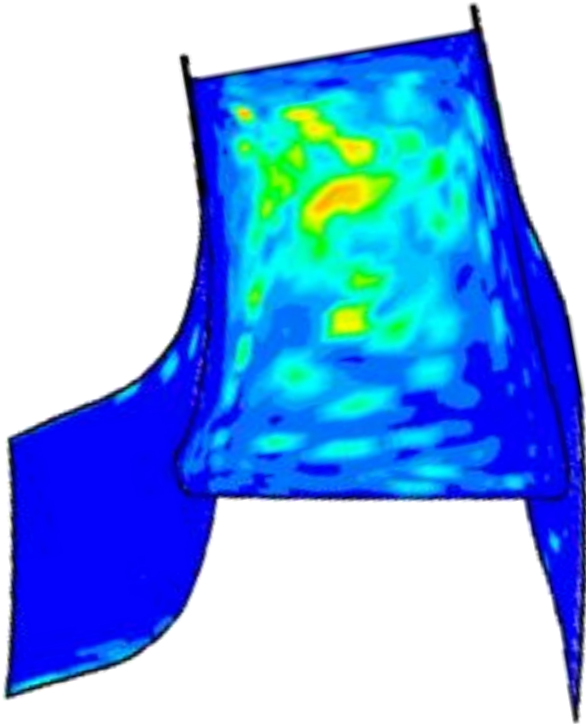
# Particle Injection

## Injection Properties

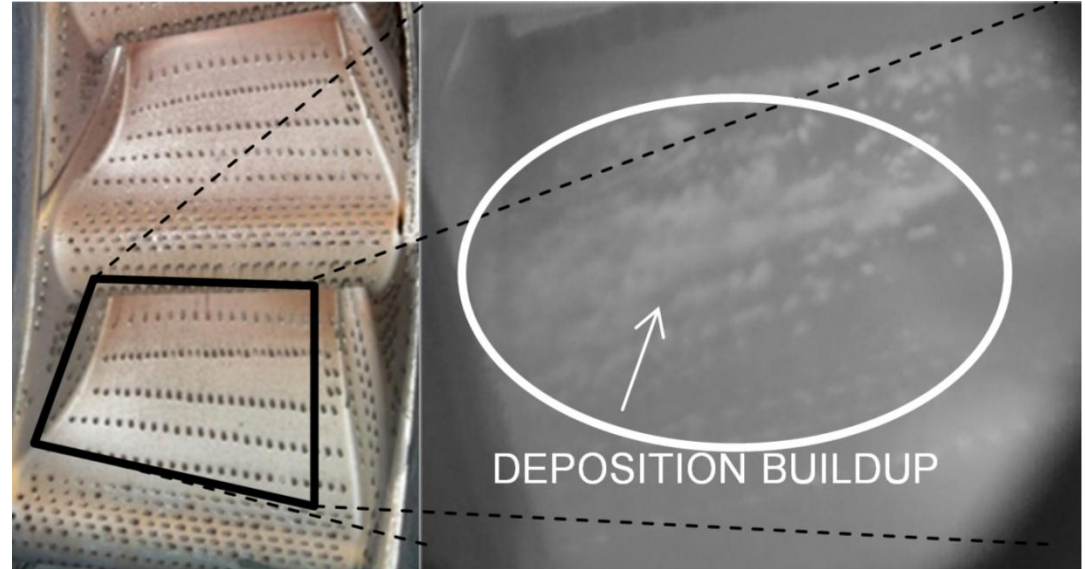
- Particles injected from several locations dispersed across inlet
- Assumes uniform distribution of particulate
- Assumes particles are in equilibrium with flow (i.e. thermal and local velocity)



# Model Verification



Critical Viscosity Model



Video from Experiment shows that initial deposition growth occurs as predicted by model.

# Why Hot Streaks?

Studying the effects hot streaks have on deposition leads to better fidelity modeling

- Deposition has a strong dependence on temp. thus H.S. in vane passages can lead to additional deposition.
- They play an important role in the unsteady rotor passage flow and heat transfer.
- HS can affect film cooling: both removing cooling from where one hopes it would go AND necessitating more cooling in regions where the HS passes close to the surface

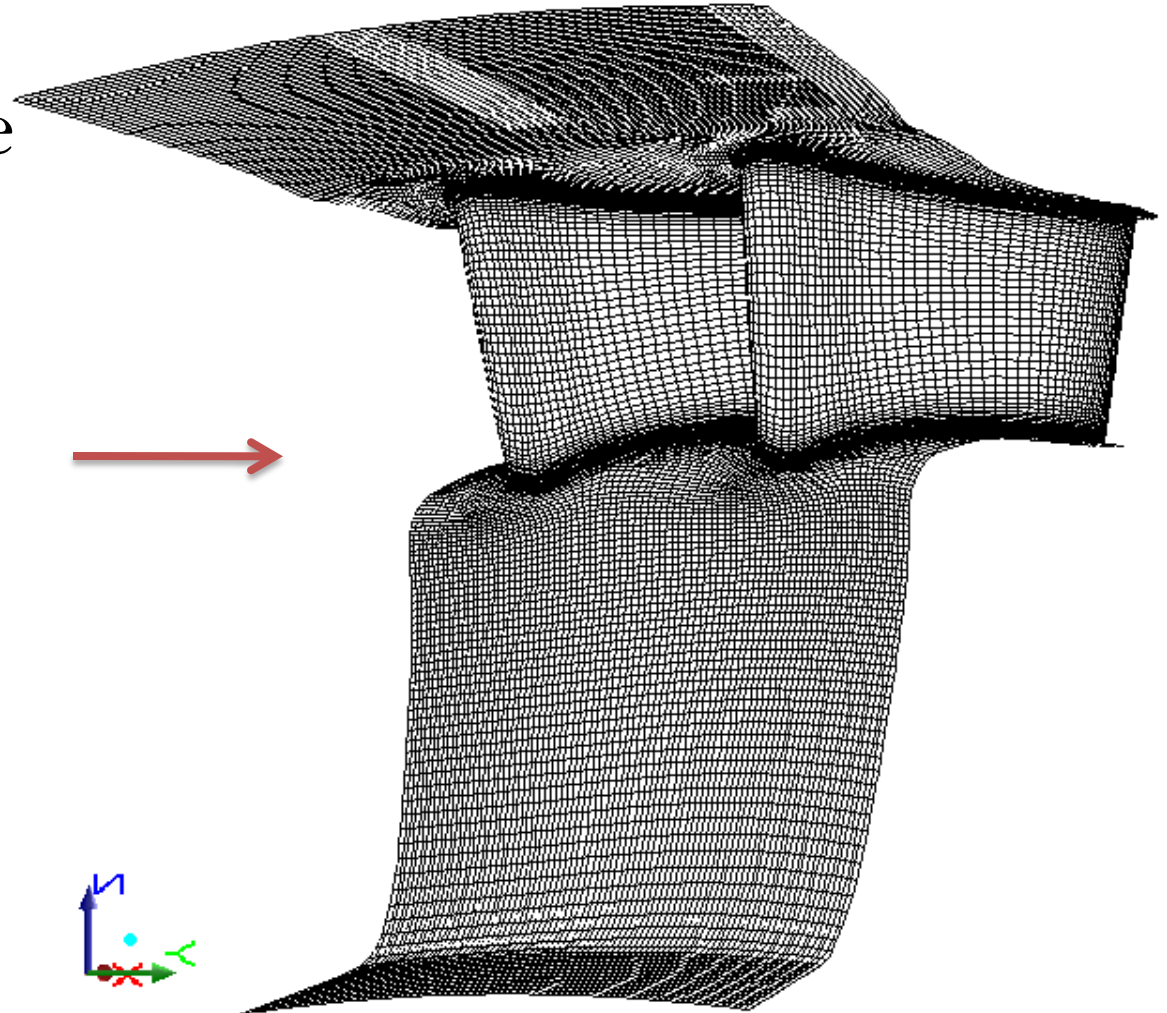
# Hot Streak Model

Studied deposition growth on a 3D turbine vane with Hot Streaks

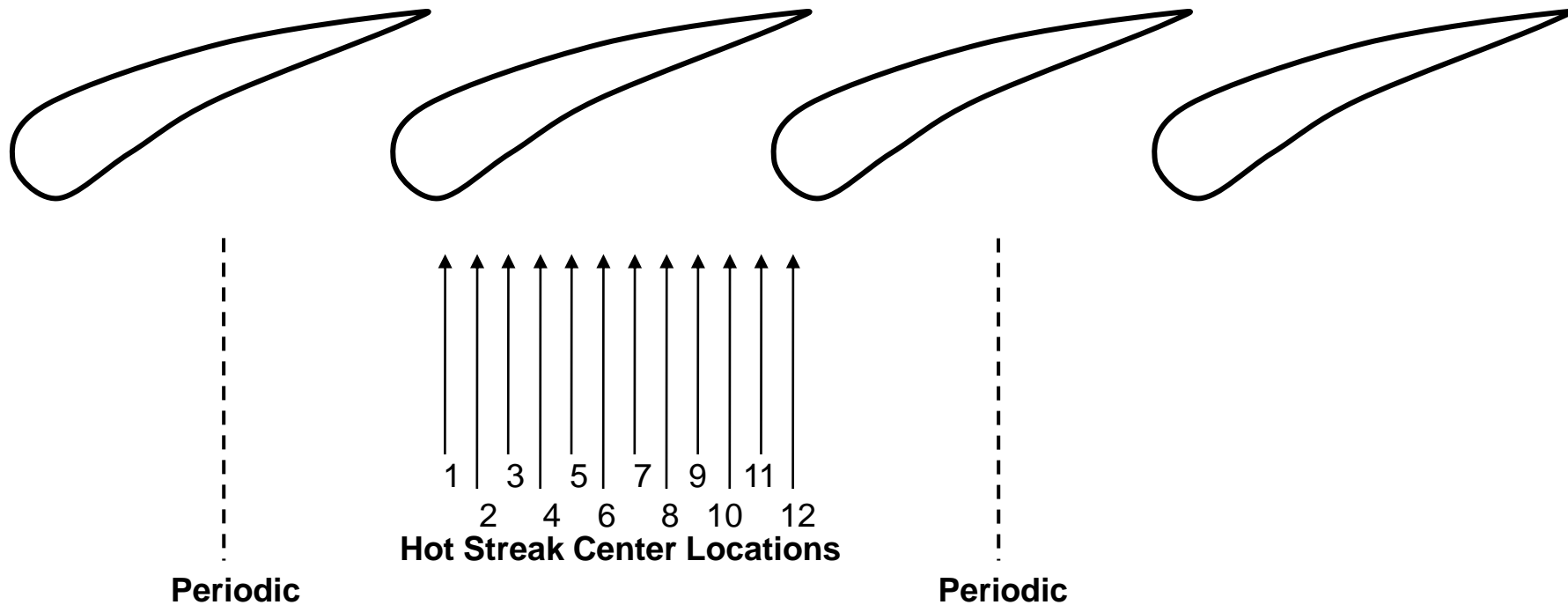
- Hot streak profiles
  - Axisymmetric profiles (w.r.t combustor axis)
  - Gaussian temp. variation (peaking at center)
  - Flat Turb. Profile of 5% (Gaussian future study )
- Hot streaks arranged (24 hr. Clock) with a two vane pitch between the streaks.
- Use E<sup>3</sup> Vane Model (Aero-Engine)

# Geometry and Grid

GE- E<sup>3</sup> HP-Vane  
Extended inlet

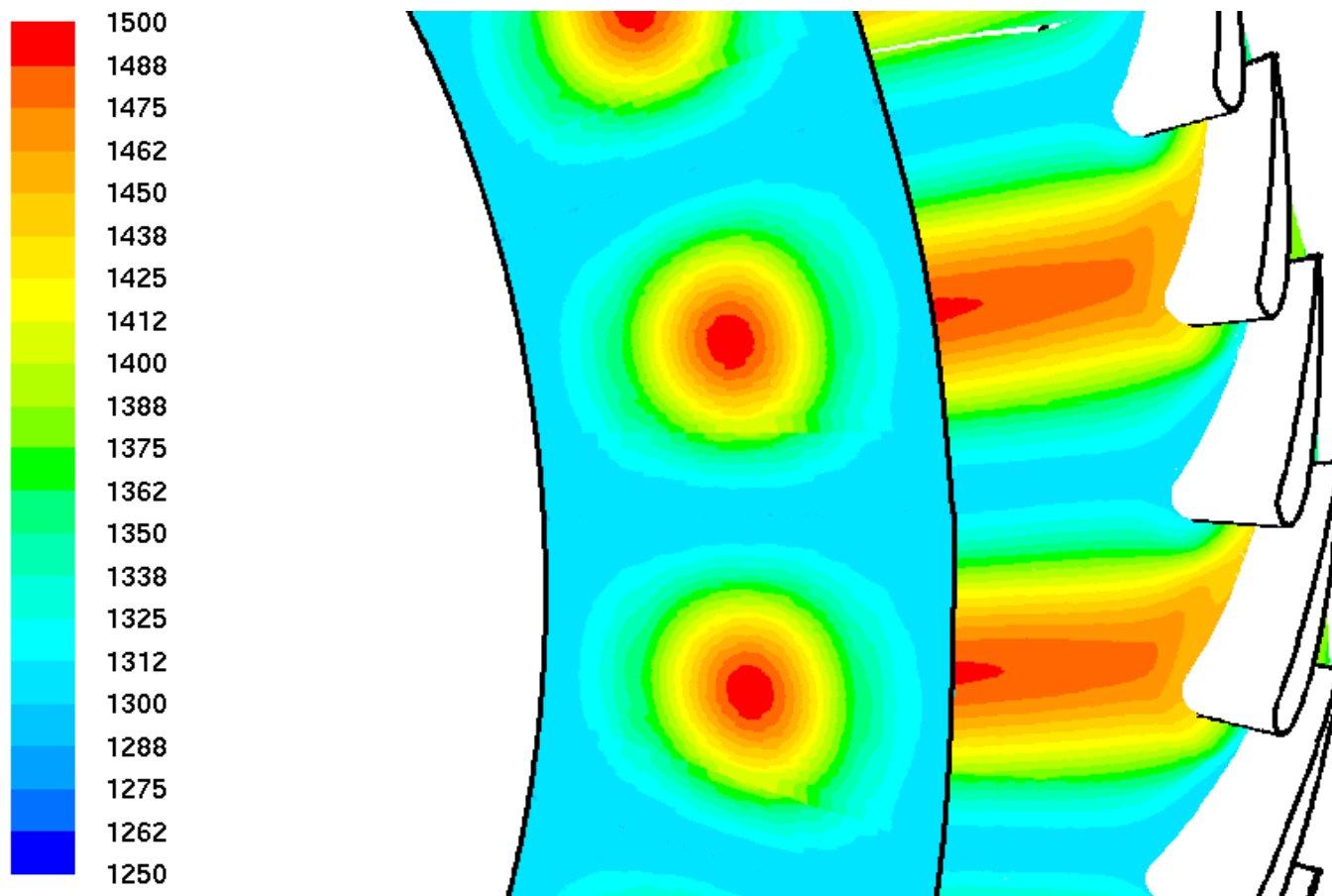


# Hot Streak Position Diagram



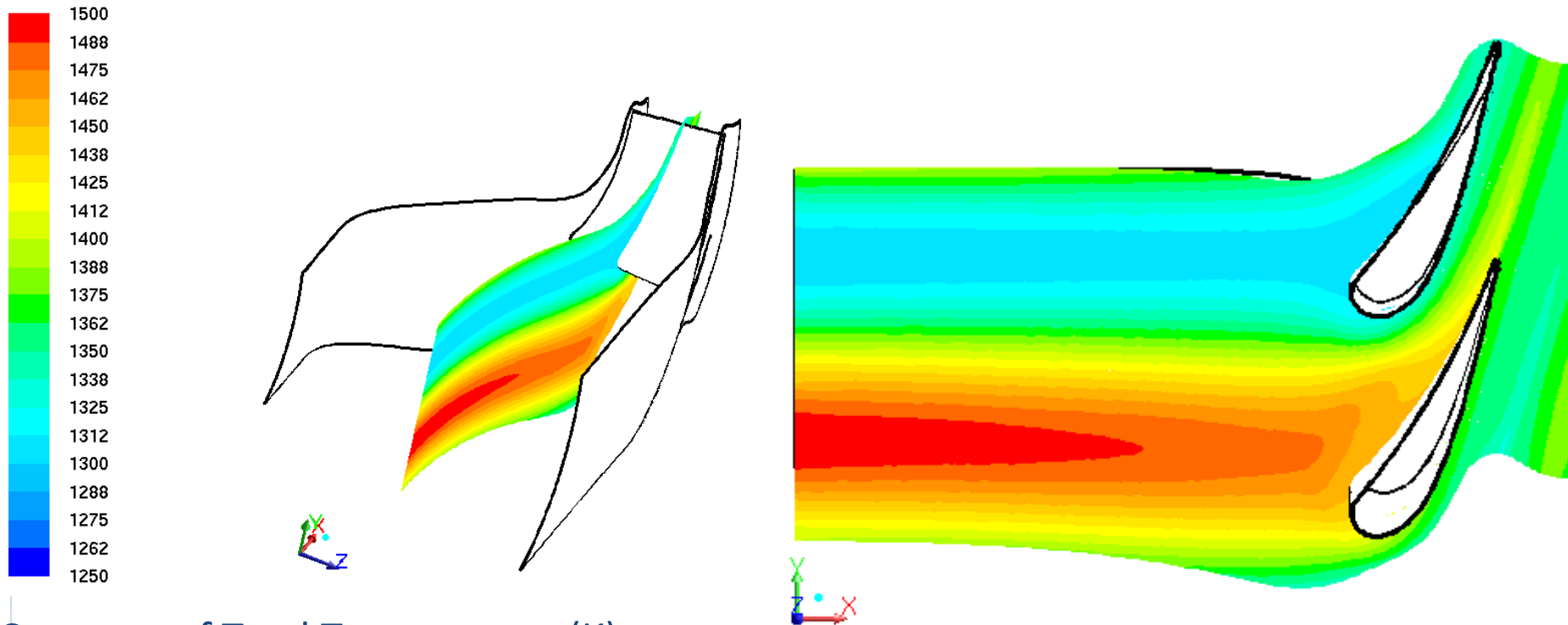


# Hot Streak Inlet Temperature Profiles



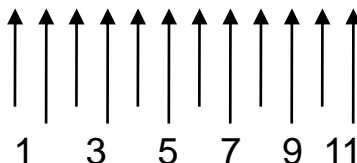
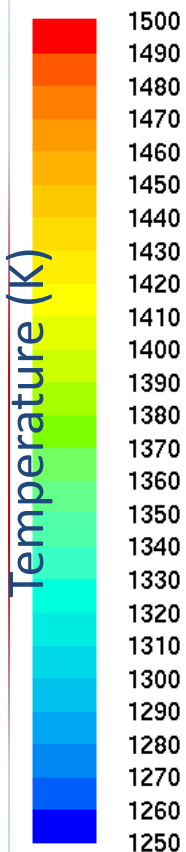
- One Streak per vane doublet.

# Hot Streak Coherence

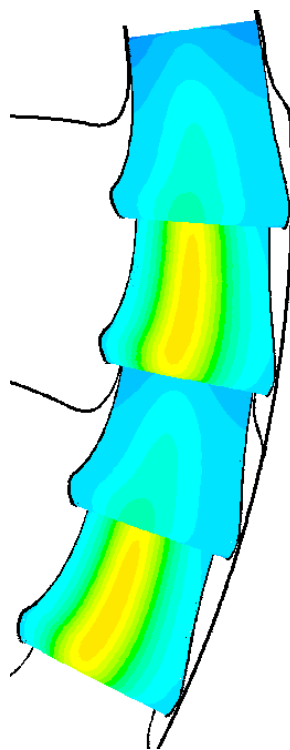


Contours of Total Temperature (K)

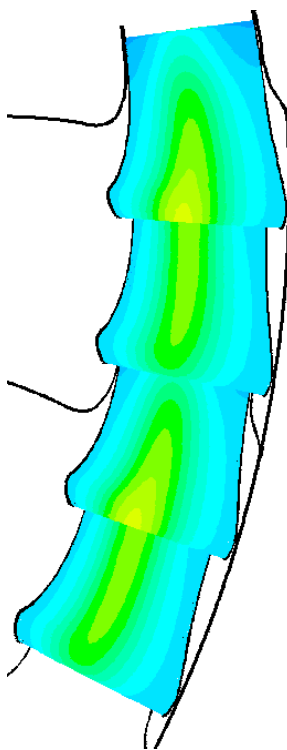
# Surface Temperature Profiles



Clock - 1



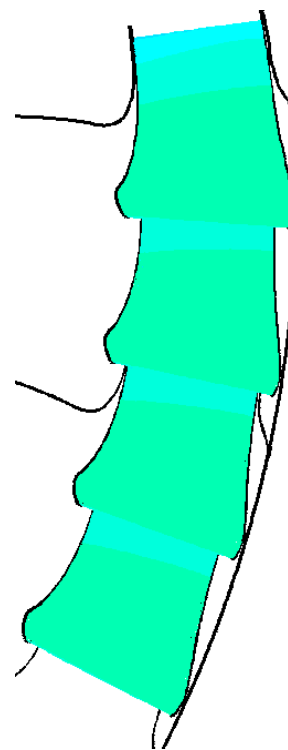
Clock - 4



Clock - 7



Clock - 10



Uniform Inlet

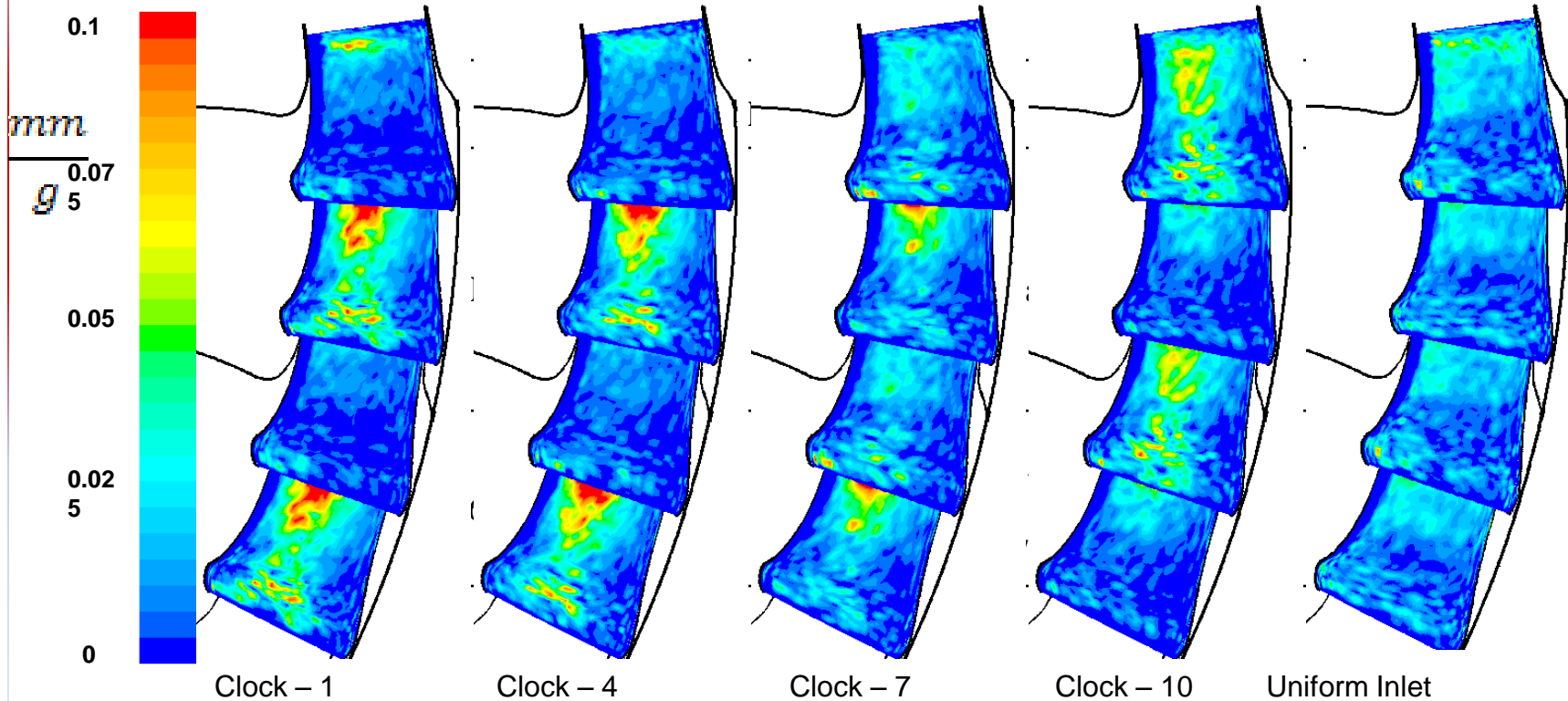
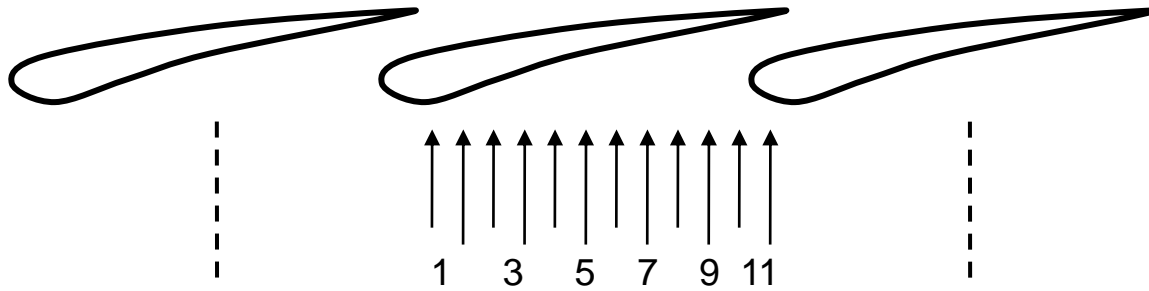
# Deposition Modeling

- Used JBPS Ash composition.

Mass Mean Diameter	Bulk Density	Element Weight %											
		Na	Mg	Al	Si	P	S	K	Ca	Ti	V	Fe	Ni
13.4 $\mu\text{m}$	2.32 g/cc	6.9	3.6	18	47	1.6	1.8	2.6	8.7	1.6	0	6.4	0

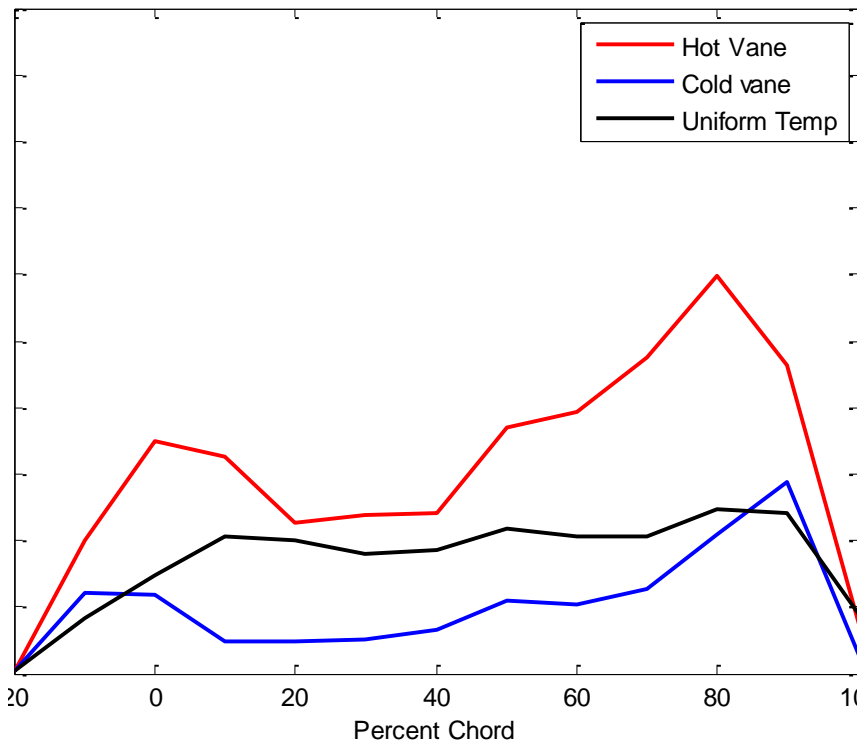
$C_p$ (J/kg-K)	K(W/m-K)
984	0.5

# Deposition Locations

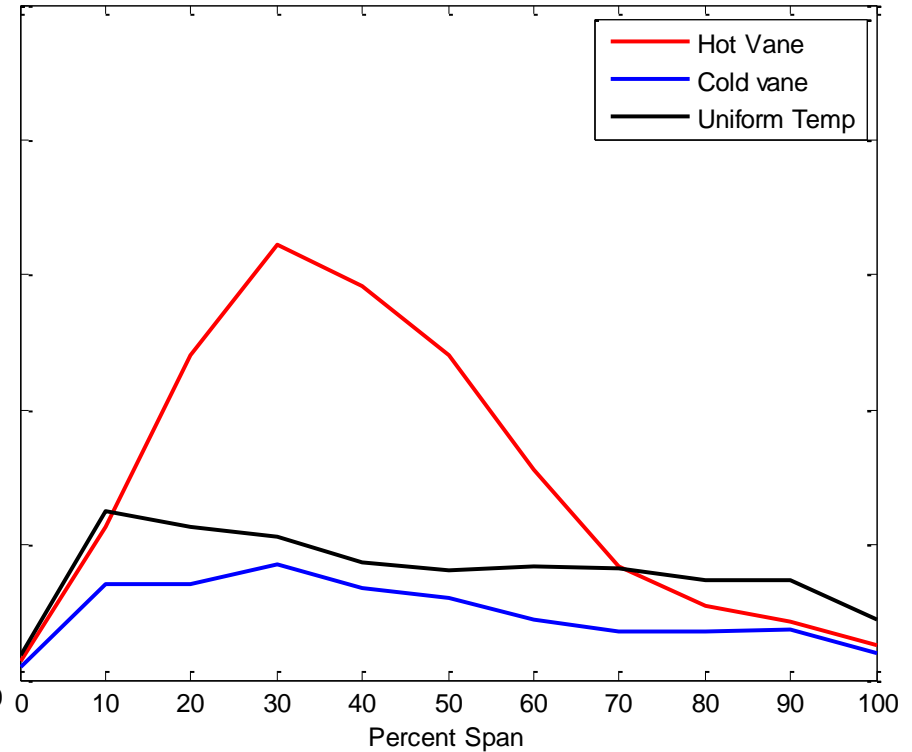


# Chord/Span Integrated Deposition

At 1 o'clock position

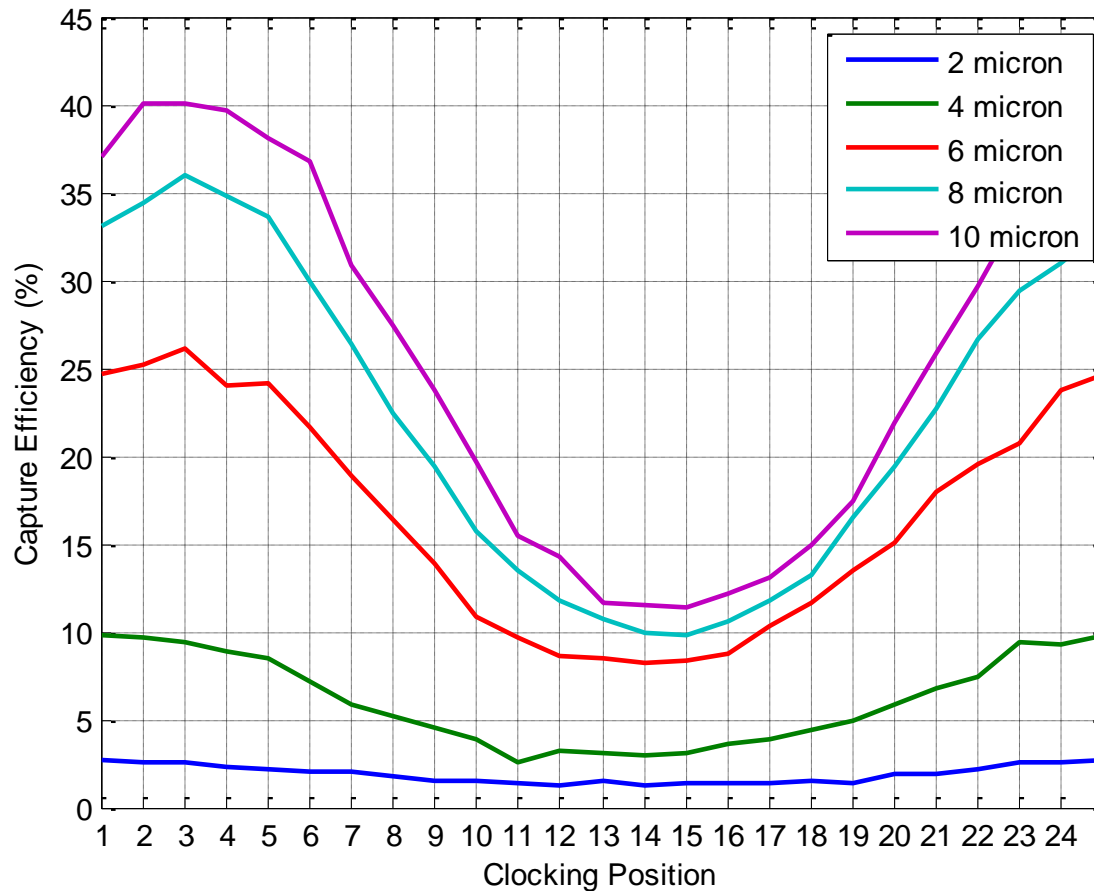


spanwise averaged  
deposition



chordwise averaged  
deposition

# Capture Efficiency Plot

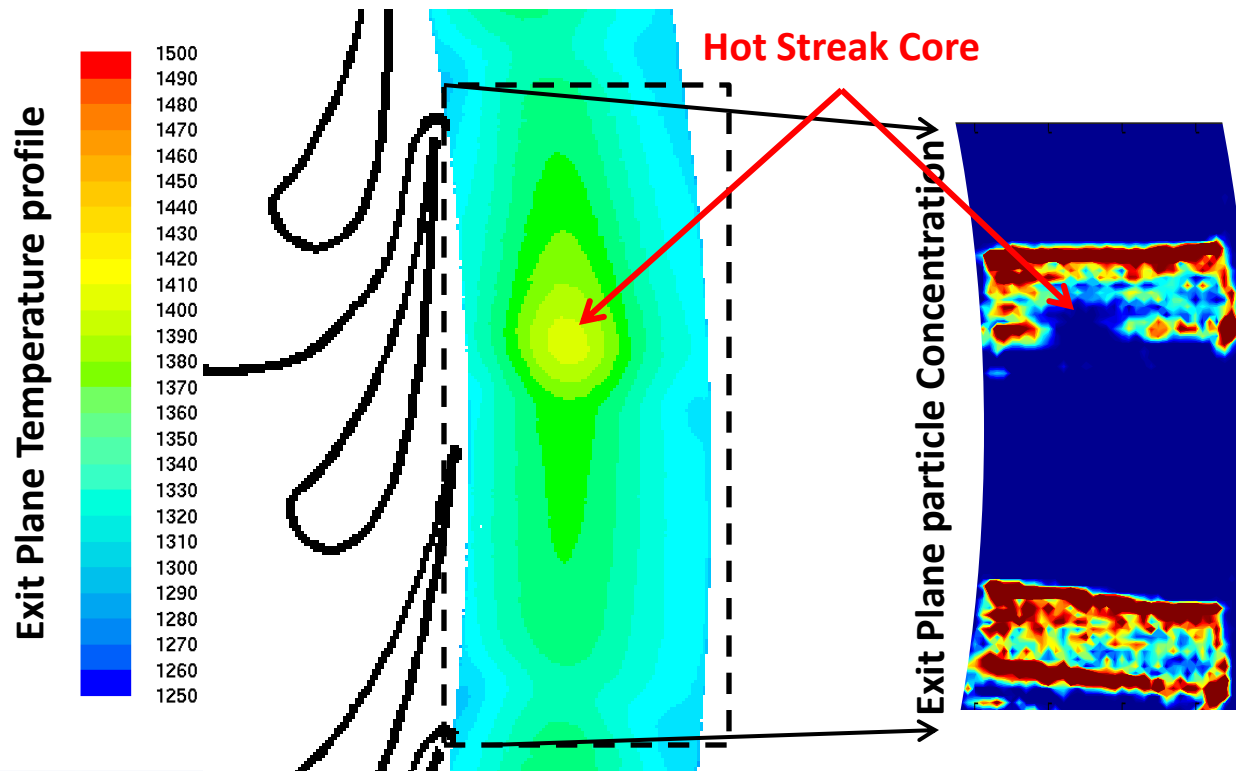


Capture efficiency defined as total deposition on single vane divided by half of particulate injected into vane doublet geometry



# Exit Plane Particle Concentration and Temperature(1:00 o'clock)

- Particulate is concentrated in layers corresponding to trailing ends of vanes
- Particulate is absent in hot streak core (particulate deposited on vane)



# Conclusions of Preliminary Study

- For the turbulence level attempted, hot streaks survive the vane passages.
- The relative position (and count ratio) of H.S. w.r.t. to the vanes affect the deposition patterns.
- The relative position of H.S. w.r.t. to the vanes affect particulate content of the flow downstream of the vanes.
- The effect of H.S. on deposition is strongly related to the Stokes number.

# Effect of H.S. on Blades

***It has been previously observed that:***

- Hot gases from the streaks migrate to the pressure side while cooler gases accumulate on the suction side.
- Position of hot streaks with respect to the vane impacts the migration path through the rotor passage and heat transfer
- Buoyancy causes the hot gases to sink to the roots of the blades
- Film cooling is made difficult by the action of H.S. not following expected streamlines.

# Blade Heat Transfer

- Hot Streaks modify wall heat transfer by both modifying the flow field and imposing a higher thermal potential on blades.
- Effect on heat transfer may not be described by the adiabatic wall temperature distribution alone.
- Heat transfer coefficient, defined properly, can show the effect of the hot streak on the blade heat transfer.
- We may be able to define  $h$ , heat transfer coefficient that is flow dependent;  $h = q_w / (T_{aw} - T_w)$  for a given form of hot streak.

# Further Details

- Unsteady  $h$  may be computed by:
  - **Using an Isothermal Condition to get  $Q_{\text{wall}}$**
  - **Using an adiabatic condition to get  $T_{\text{aw}}$**
  - **using a phase locked condition**
  - **$h = Q_{\text{wall}} / (T_{\text{aw}} - T_w)$  and then averaged.**
- For uniform inlet, heat transfer can be computed in the same manner.
- The effect of the hot streak can be discerned from the difference.

# GTL's Relevant Cases

- Experiments on 1 ½ stage HP turbines were conducted at OSU GTL
- Both uncooled vane and cooled vane.
- Hot Streak targeted at mid-pitch or vane leading edge
- Hot Streak intensity varied
- Cooling rate varied
- $Q_{\text{wall}}$  measured

**We will use the data sets pending access.**

# GTL's Relevant Cases

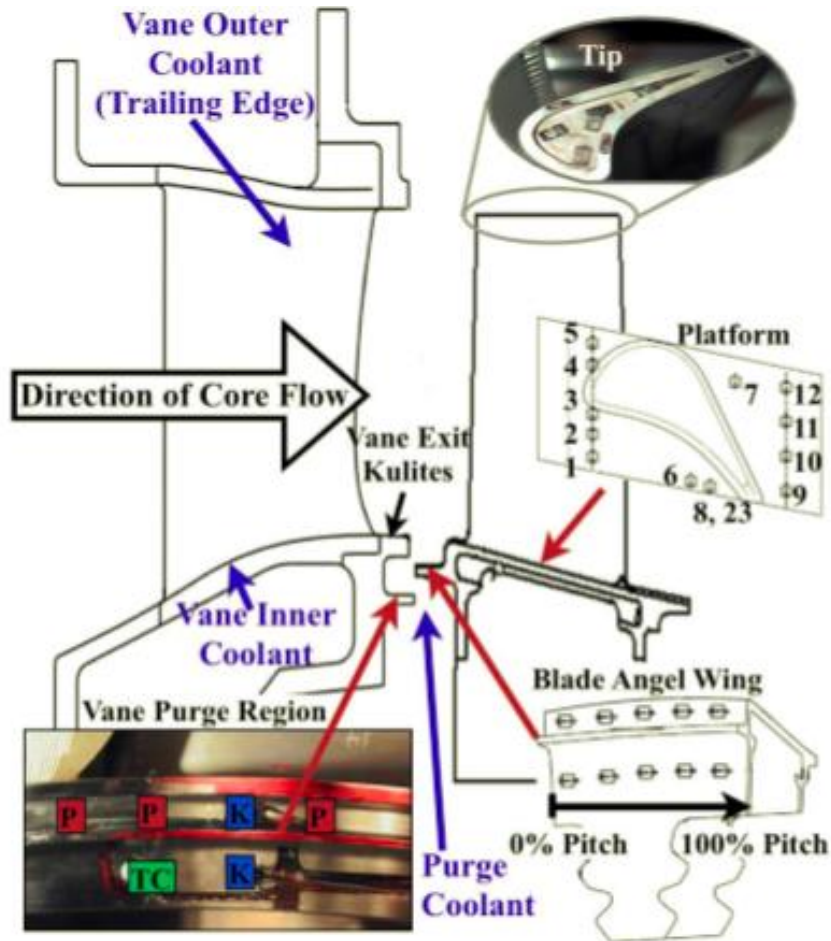


Figure 1. Schematic of instrument locations (not to scale)

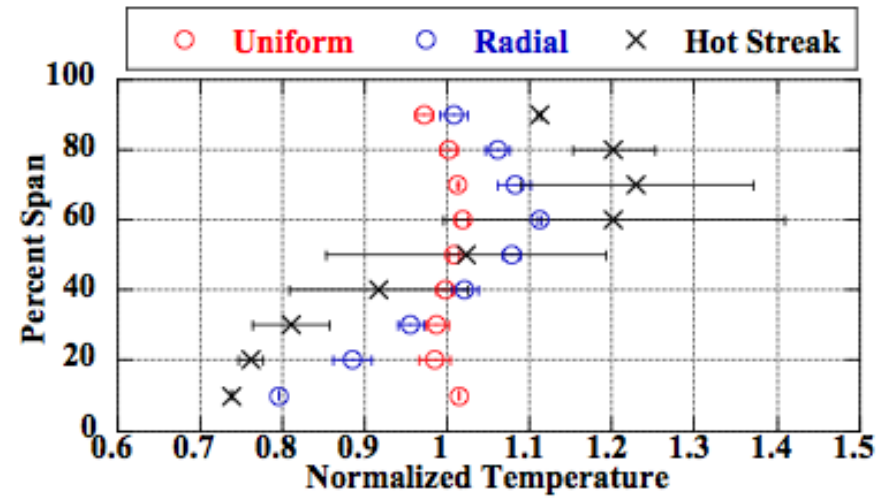


Figure 2. Comparison of inlet temperature profile shapes for runs without cooling



# GTL's Relevant Cases

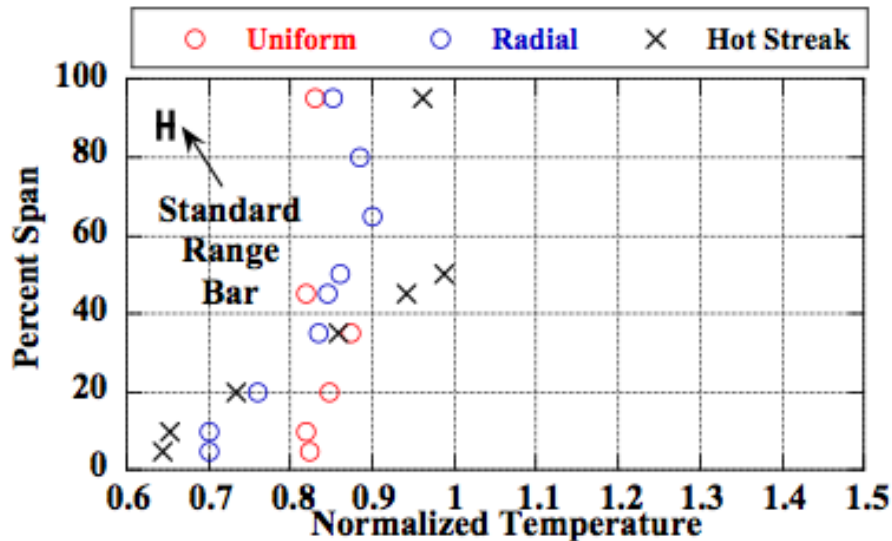


Figure 3. Comparison of rotor inlet temperature profiles measured by blade leading edge thermocouples for runs without cooling

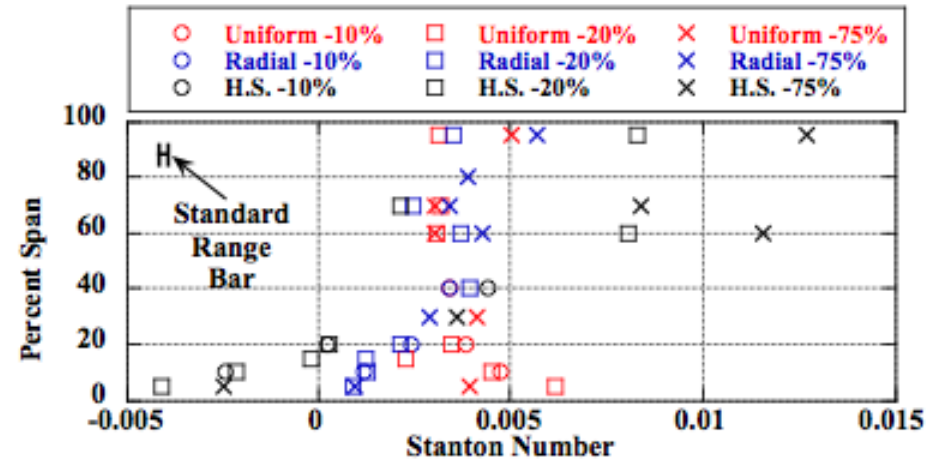


Figure 4. Stanton Number distributions for pressure surface with different inlet temperature profile shapes

# Deposition Modeling

- Critical Viscosity Model
  - probability of sticking exclusive function of particle viscosity and thus  $f(\text{Temp})$  ONLY.
  - NO sensitivity to particle size, impact velocity or angle of impingement
  
- Critical Velocity Model
  - particle sticks IF normal velocity  $<$  critical velocity
  - critical velocity is  $f(\text{size, Youngs Modulus, Poissons ratio})$
  - Youngs Modulus is  $f(\text{Temp})$
  - DOES NOT model plastic deformation!!!

# Critical Viscosity Model

Motivated by the observed trend that the Adhesion Efficiency of small (53-74 $\mu$ m) microspheres increases as Temperature increases and viscosity decreases!

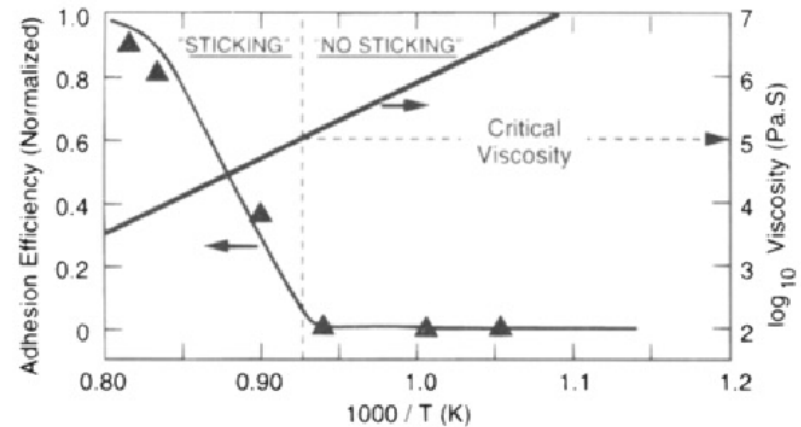


**Figure 1.** Adhesion efficiency and viscosity of soda lime glass spheres impacting on a horizontal tube as a function of temperature.

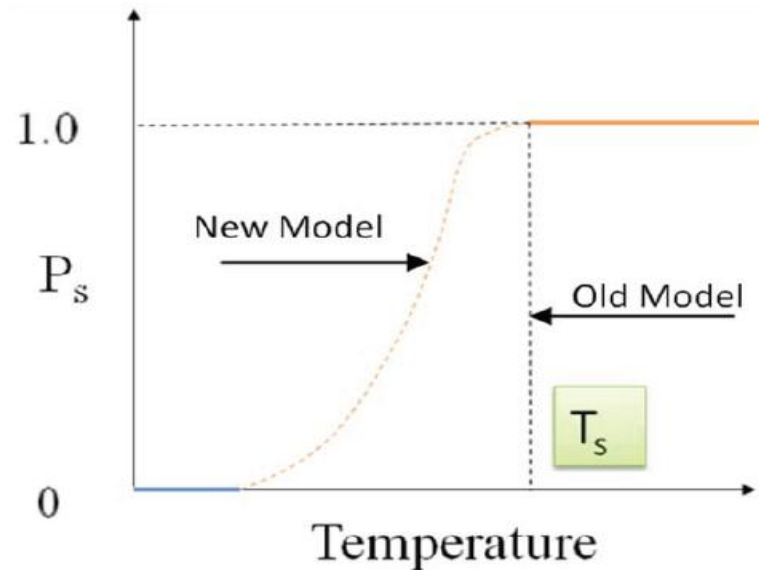
SRINIVASACHAR, S. "An experimental study of the inertial deposition of ash under coal combustion conditions." *Symposium (International) on Combustion*, v. 23 issue 1, 1991, p. 1305-1312.

Lower viscosity means that the particle is more likely to “flow” (i.e. deform) upon impact with the surface. This is **PLASTIC** deformation. As the particle plastically deforms, the contact area with the surface increases and thus the adhesion force (proportional to contact area) increases.

# Critical Viscosity Model

Sreedharan, S.S., Tafti, D.K., 2010. Composition dependent model for the prediction of syngas ash deposition in turbine gas hotpath. International Journal of Heat and Fluid Flow Volume 32, Issue 1, February 2011, Pages 201-211

Based on these observations, Tafti and Sreedharan (IGTI 2010) concluded that once the particle reaches some critical viscosity, it will ALWAYS stick to the surface.



Below this critical viscosity (or Sticking Temperature,  $T_s$ ) the probability of sticking ( $P_s$ ) could be determined using a ratio of the “critical” viscosity to the particle viscosity at temperature.

$$P_s(T_p) = \frac{\mu_{crit}}{\mu_{T_p}}$$

# Critical Viscosity Model

As such, the problem reduces to finding  $T_s$  and  $\mu(T)$

For pure substances,  $\mu(T)$  can be found experimentally using a viscometer and  $T_s$  can be found by heating a cube of material until it softens and deforms.

Ash particulate is composed of a variety of inorganic compounds depending on the type of ash that it being used. The strength of the bonds that these compounds form can be used to estimate viscosity, or how easily it can PLASTICALLY deform. (Empirically based on ratios of glass formers to modifiers, Senior and Srinivisachar [1995])

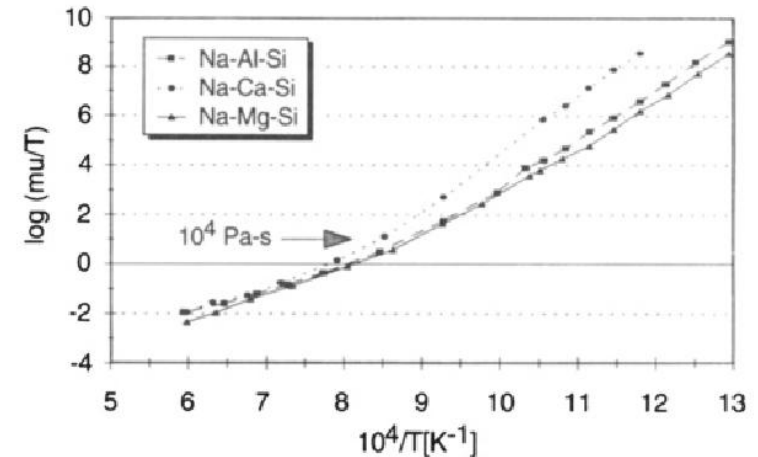
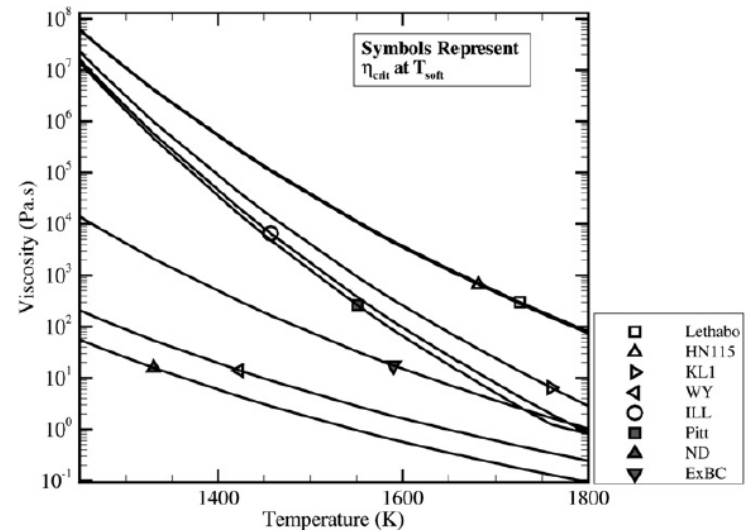
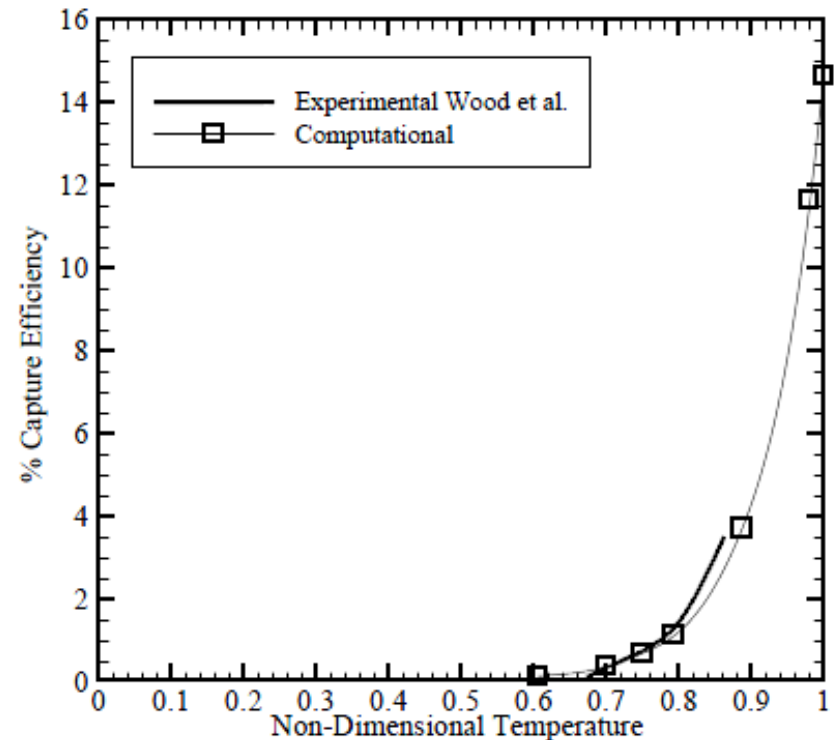


**Figure 2.** Viscosity as a function of temperature for silicate glasses: (■)  $\text{Na}_2\text{O}-\text{Al}_2\text{O}_3-\text{SiO}_2$ , (●)  $\text{Na}_2\text{O}-\text{CaO}-\text{SiO}_2$ , (▲)  $\text{Na}_2\text{O}-\text{MgO}-\text{SiO}_2$  (source: ref 23).



# Critical Viscosity Model

Using the model of Senior and Srinivasachar, Tafti and Sreedharan estimated the  $T_s$  and  $\mu(T)$  distribution for their ash and compared their predicted capture efficiency to the experiment of Wood et al. (24  $\mu\text{m}$  PVC particles) and found reasonable agreement.



Sreedharan, S.S., Tafti, D.K., 2010. COMPOSITION DEPENDENT MODEL FOR THE PREDICTION OF SYNGAS ASH DEPOSITION WITH APPLICATION TO A LEADING EDGE TURBINE VANE. ASME Paper No. GT2010-23655

**Wood et al. (IGTI 2010) 24micron PVC particles with  $T_s = 533\text{K}$  (Stokes=0.12)**

# Critique of the Critical Viscosity Model

- Viscosity influences the amount of plastic deformation that occurs for a given impact condition – the greater the plastic deformation, the higher the propensity for sticking!
- The energy required to plastically deform the particle comes from the KINETIC ENERGY at impact.
- Kinetic energy is a function of velocity and size (mass) of the particle.



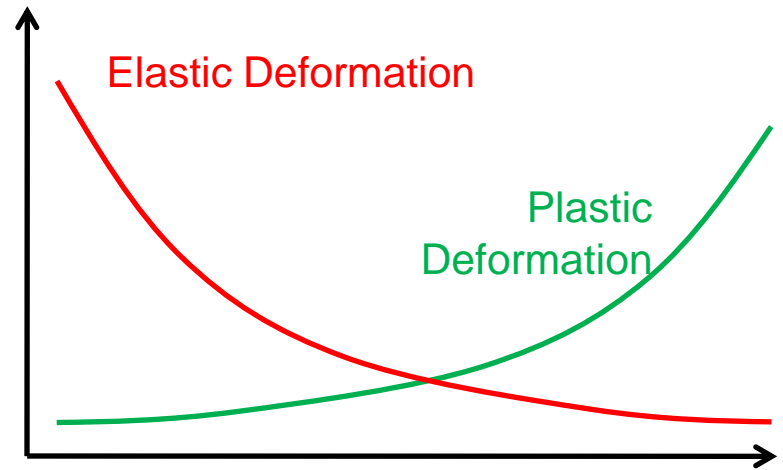
Thus, the probability of sticking should also depend on impact velocity and particle size.



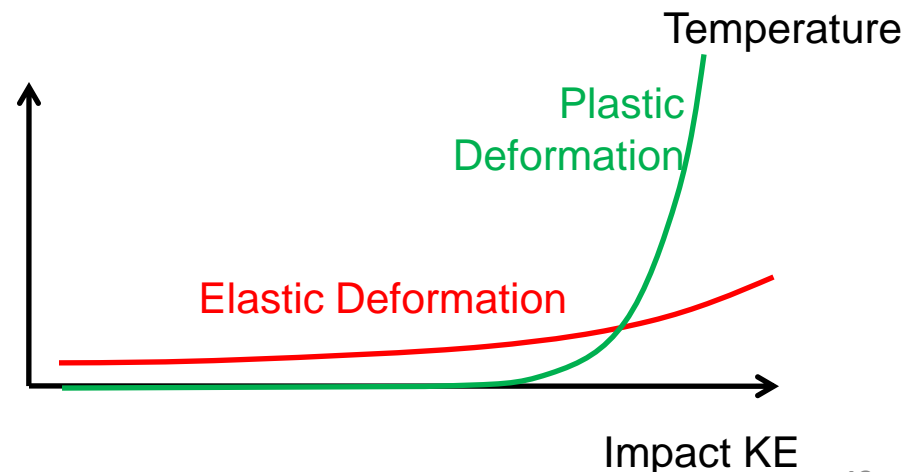
# Critique of the Critical Viscosity Model

Upon impact, the particle experiences BOTH elastic and plastic deformation.

Amount of each deformation will no doubt depend on structural mechanics ( $E$  or  $\mu$ ), which are both functions of temperature.

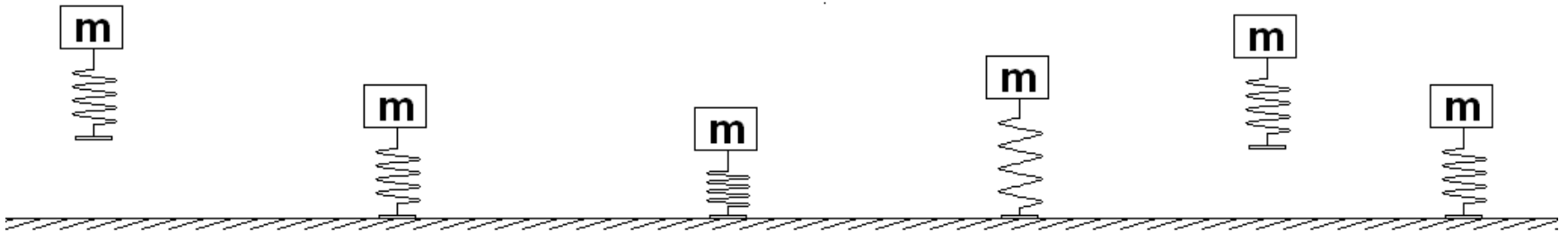


But it will also depend on impact kinetic energy (e.g. clay projectile)



# Critical VELOCITY Model

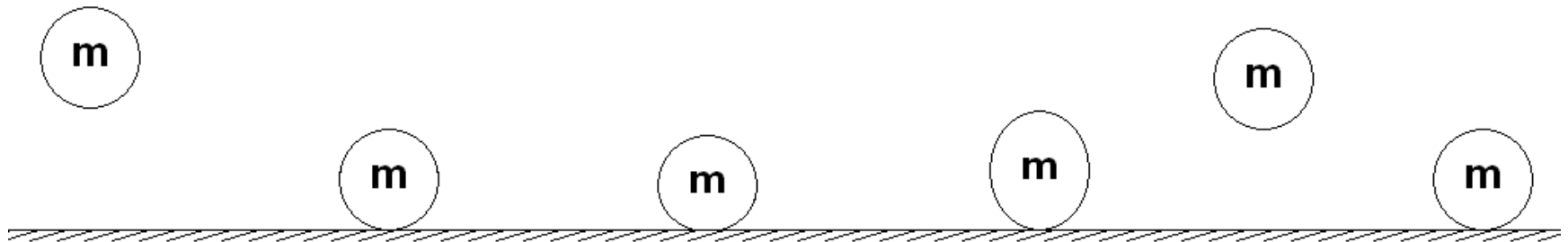
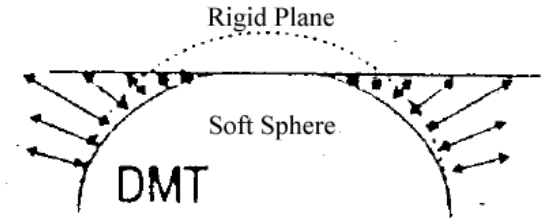
Motivated by the observed trend that the rebound of small particles requires some minimum energy to overcome adhesion force!



- Particle represented by mass, spring, and contact platform.
- Upon contact, spring compresses.
- Compressed spring releases energy propelling particle from wall
- Adhesion force on contact platform causes slight tension of spring before RELEASE or CAPTURE.
- (Simplified model has constant contact area.)

# Critical VELOCITY Model

Hertzian contact mechanics predict increased contact surface area due to ELASTIC deformation upon impact!

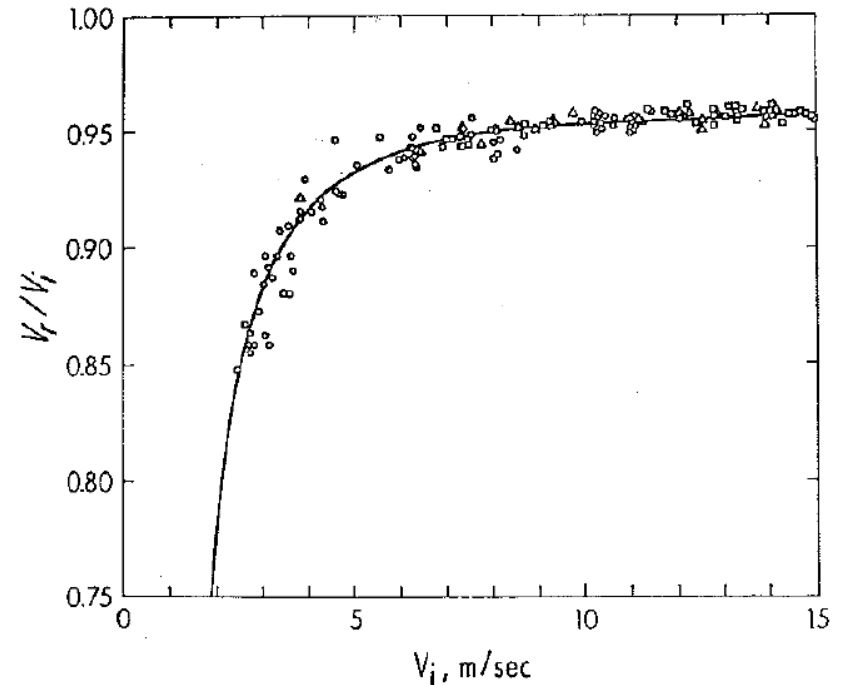


- Particle represented by elastic sphere
- Upon contact, sphere deforms.
- Energy stored in compression propels particle from wall
- Adhesion force on contact surface area causes slight tension of particle before RELEASE or CAPTURE.
- Contact surface area varies with time.

# Critical VELOCITY Model

## Effect of particle SIZE

- Large particles ( $d > 100\mu\text{m}$ )
  - Almost perfectly elastic collisions at low velocity.
  - Coefficient of restitution ( $R$ ) decreases at high normal velocity as plastic deformation becomes significant
  
- Small particles ( $d < 100\mu\text{m}$ )
  - Similar to large particles EXCEPT at low velocities ( $< 10\text{m/s}$ )
  - At low velocities, adhesion forces due to electrostatic and van der Waals forces cause  $R$  to decrease dramatically!



Ratios of final-to-initial normal velocities *from impacts of microspheres* ( $1.27\ \mu\text{m}$  diameter) against a flat surface

Dahneke, B. (1975). *J. Colloid Interface Sci.* 51:58-65.

# Critical VELOCITY Model

Brach and Dunn (ND, 1992) developed a model to estimate the work required to overcome the adhesion force ( $W_A$ ). The model is based on particle kinematics and ONLY accounts for elastic deformation.

$$W_A = - \left[ \frac{5}{4} \rho \pi^2 (k_1 + k_2) \right]^{\frac{2}{5}} r^2 \gamma v_n^{\frac{4}{5}}$$

$$W_A = \frac{1}{2} m v_n^2 \left( \frac{V_n^2}{v_n^2} - R^2 \right)$$

$W_A$  is a function of:

- particle properties ( $k_1$  is function of Youngs Modulus and Poisson Ratio)
- surface properties ( $k_2$  is function of Youngs Modulus and Poisson Ratio)
- size ( $r$  is sphere radius)
- surface energy adhesion parameter ( $\gamma$ )
- normal impact velocity ( $v_n$ )
- coefficient of Restitution ( $R$ )
- mass ( $m$ )
- normal release velocity ( $V_n$ )

2 equations, 3 unknowns

Requires empirical estimate for  $R$

- Fit coefficients  $k$  and  $p$   
 - Example: for NH4FI spheres,  $k=45.3$  and  $p=0.718$

$$R = \frac{k}{k + |v_n|^p}$$

# Critical VELOCITY Model

Brach and Dunn (UND, 1992) compared kinematic impact model with experimental data and developed empirical fits.

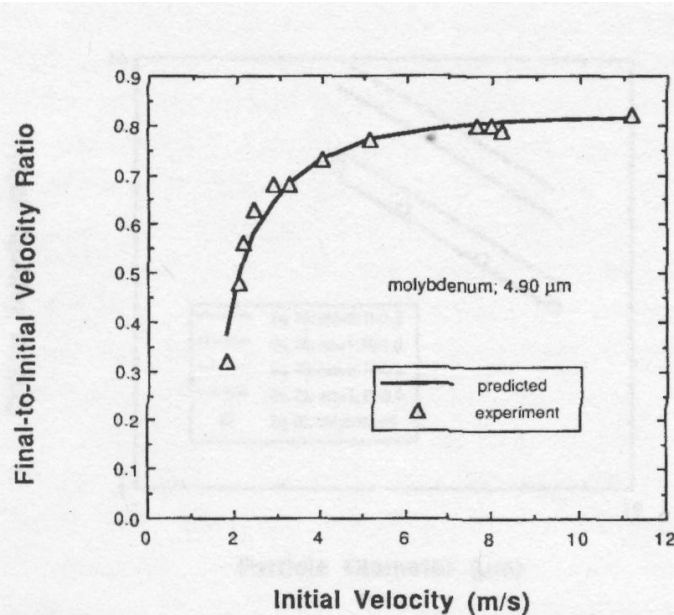


**FIGURE 3.** The final-to-initial normal velocity ratios for 4.90  $\mu\text{m}$  diameter  $\text{NH}_4\text{F}$  spheres against a molybdenum target from the data of Wall et al. (1990).

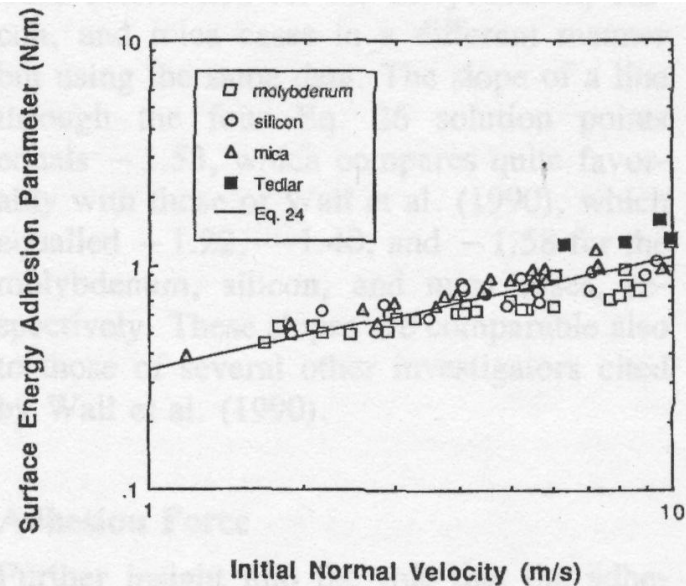
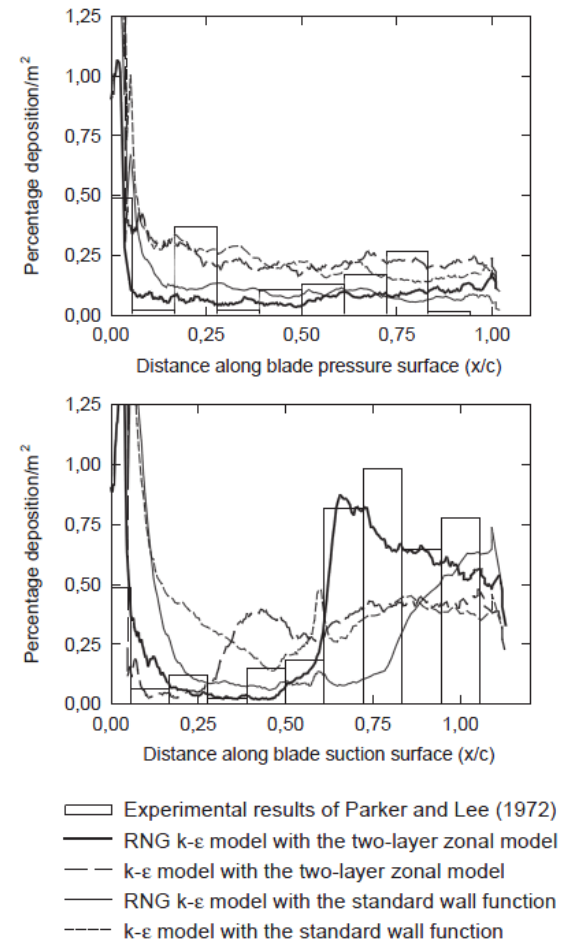


**FIGURE 4.** Values of the surface energy adhesion parameter from the data of Wall et al. (1990) for four diameters of  $\text{NH}_4\text{F}$  spheres and four target materials. The solid curve is calculated from Eq. 24.

Primarily interested in determining coefficient of Restitution and effect of ELASTIC deformation.

# Critical VELOCITY Model

- For the case of  $R=0$  (i.e. deposition), Brach and Dunn (UND, 1992) developed an expression for the critical NORMAL velocity below which particle capture was certain.
- Critical velocity is a function of particle and surface properties, particle size, mass and  $R$ .
- El-Batsh and Haselbacher (2000,2002) used this model to predict deposition in a turbine vane. Compared to experimental data of Parker and Lee (1972) – uranine particles with double-stick tape on vane.

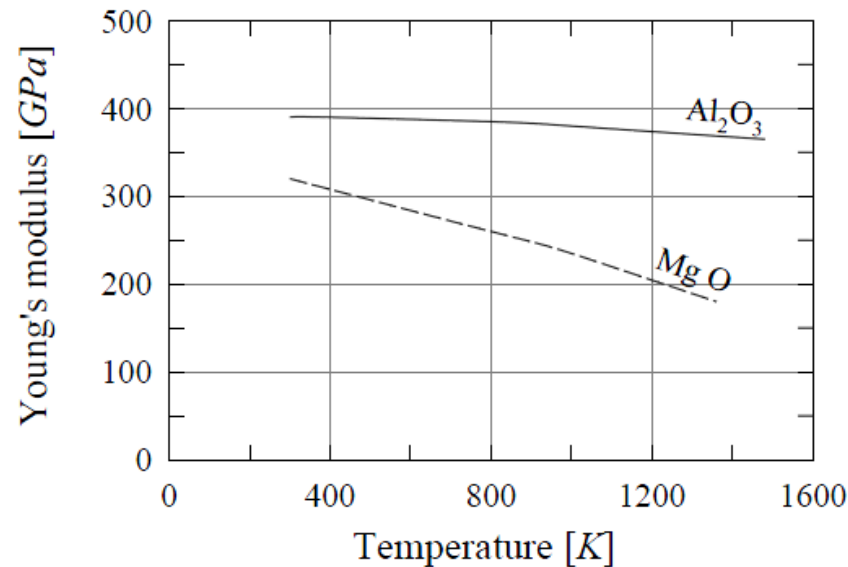


*El-Batsh, H. and Haselbacher, H. (2000), Effect of Turbulence Modeling on Particle Dispersion and Deposition on Turbine Blades, ASME paper, 2000-GT-519.*



# Critical VELOCITY Model

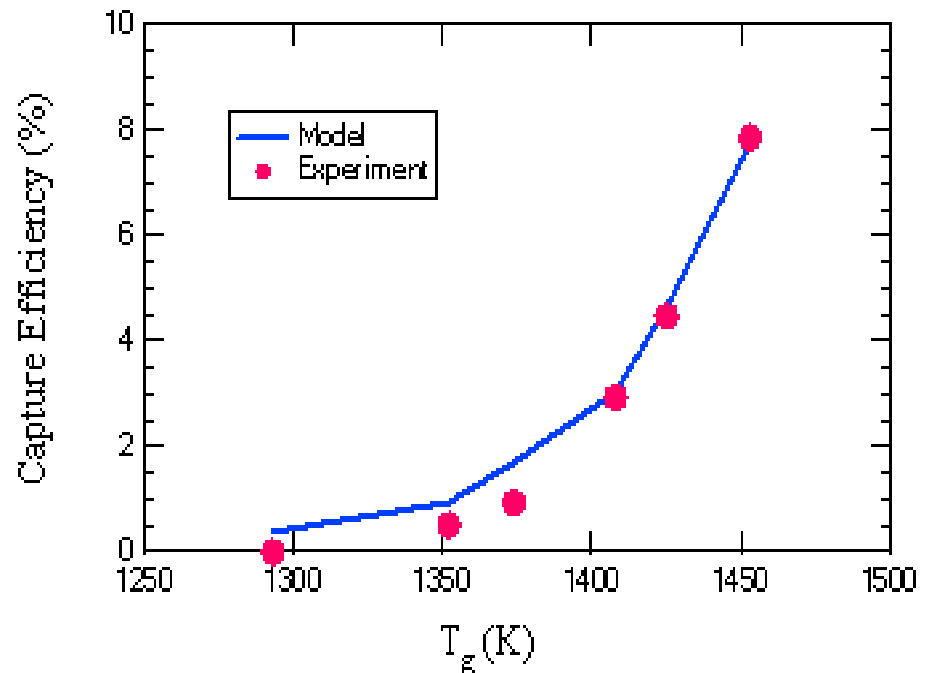
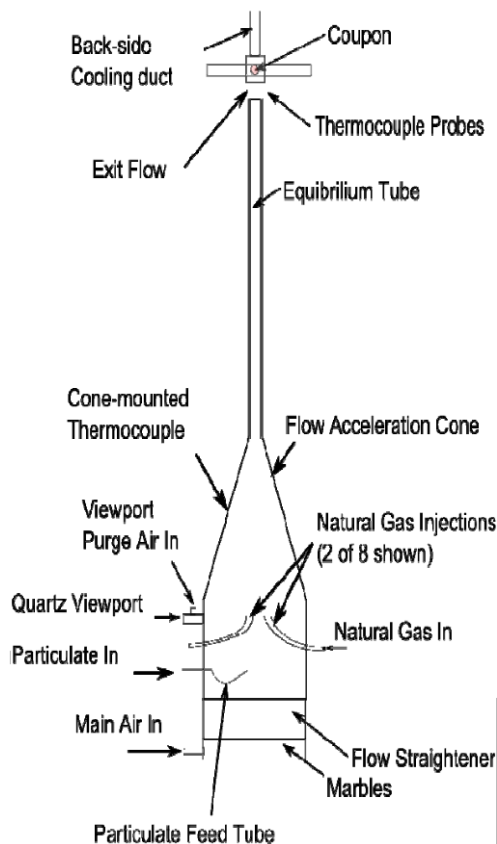
- El-Batsh and Haselbacher accounted for the variation in particle properties (E) with temperature using empirical fits to data.



Ralls, K. M.; Courtney, T. H. and Wulff, J. (1976), *Introduction to Materials Science and Engineering*, John Wiley & Sons, Inc.

# Critical VELOCITY Model

- Ai et al. (2008) used Brach and Dunn as well as El-Batsh and Haselbacher models to compare experimental capture efficiency (ash deposition) with predictions.



- 2D CFD model
- The E obtained in this model by fitting experimental data ( $T= 1293$  K to  $1453$ K)
- Dependence of Young's Modulus on temperature

# Critique of Critical VELOCITY Model

- Model includes particle kinematics, KE of impact, adhesion force, elastic deformation
- Model does NOT include **PLASTIC** deformation!

# Combination of the Models

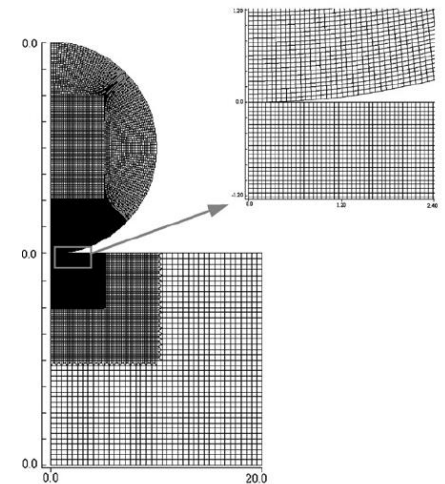
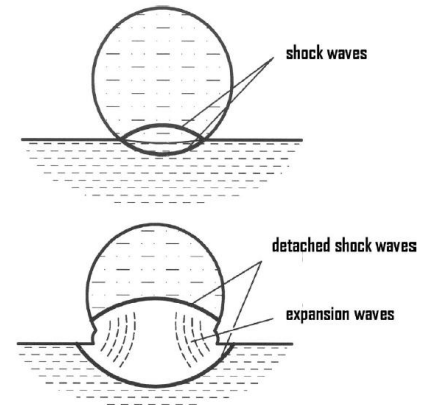
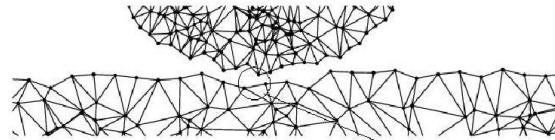
- Critical Viscosity is dependent upon the effect of plastic deformation occurring at high temperatures
- Critical Velocity is dependent upon the effect of the adhesion force occurring at lower velocities
- An impact model that incorporates both adhesion and plastic deformation would be optimal

# Combination of the Models

- The model needs to be dependent on all the outputs of CFD and known properties of the particle and the substrate
- CFD outputs
  - Particle temperature
  - Particle size
  - Particle mass
  - Particle velocity
  - Particle impingement angle
- Properties
  - Surface irregularities (roughness)
  - Modulus of Elasticity
  - Poisson's Ratio
  - Yield Stress

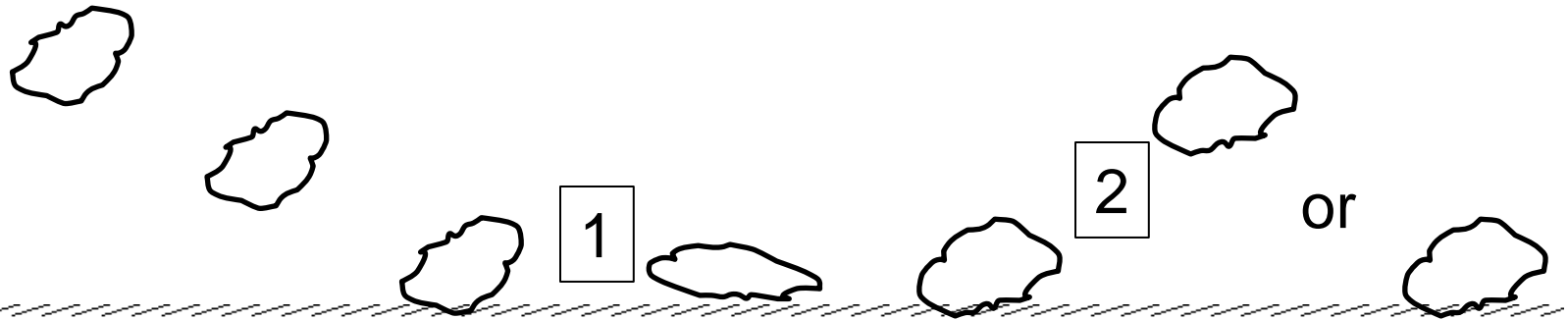
# Current Elastic-Plastic Impact Models

- Cold Spraying
  - Metal on metal impact at supersonic speeds
- Molecular Bonding
  - Attraction between the molecules of a particle
- FEM
  - Meshing particles and surfaces to simulate the impact
- Energy Methods
  - Using Energy Analysis to find final Kinetic energy
- Yield Stress determination
  - Stress over the yield, plastically deforms the particle

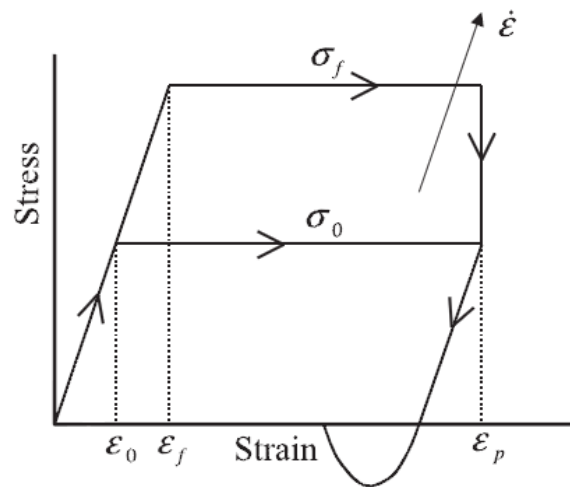


$$\begin{aligned} \text{total energy} &= E_{k_1} = \frac{1}{2}mV_1^2 \\ &= E_e + E_{pe} + E_p. \end{aligned}$$

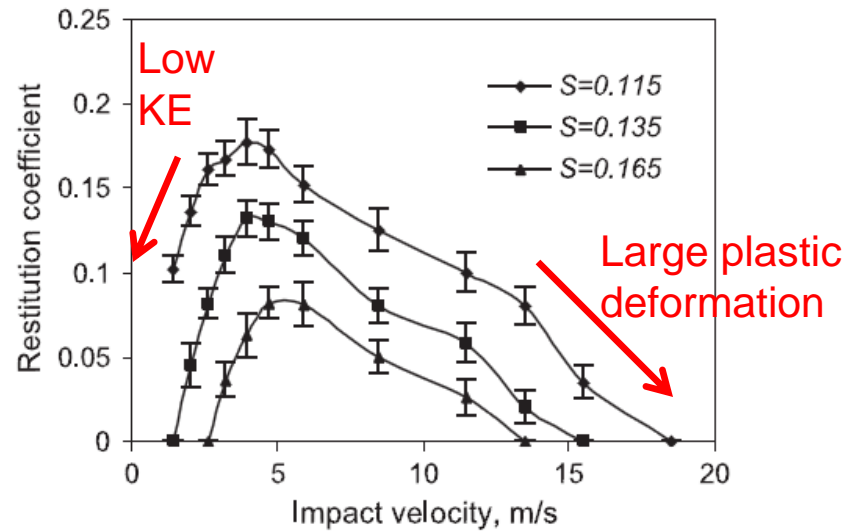
# Elastoviscoplasticity



1. Inbound kinetic energy used to elastically and plastically deform particle.
2. If residual kinetic energy exceeds work required to overcome surface adhesion – particle detaches.



Yield stress is dependent on rate of strain.



Calcium carbonate powder - 10-50 $\mu$ m.  
S is liquid to solid ratio.

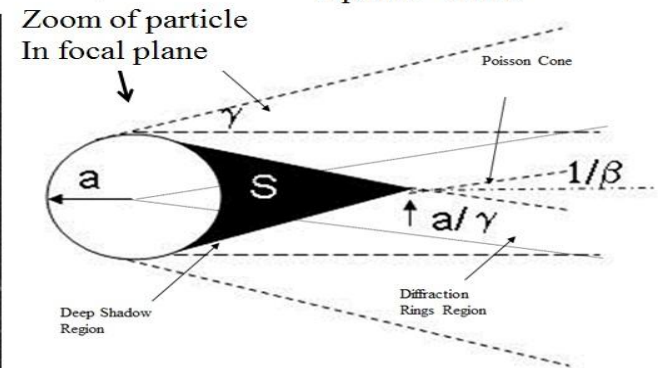
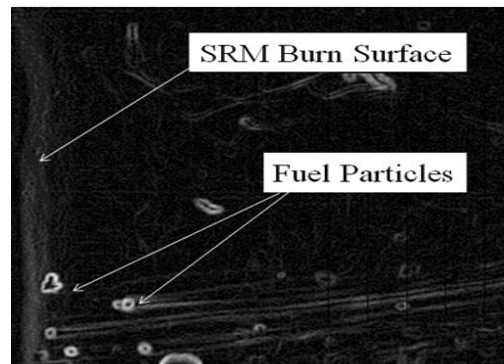
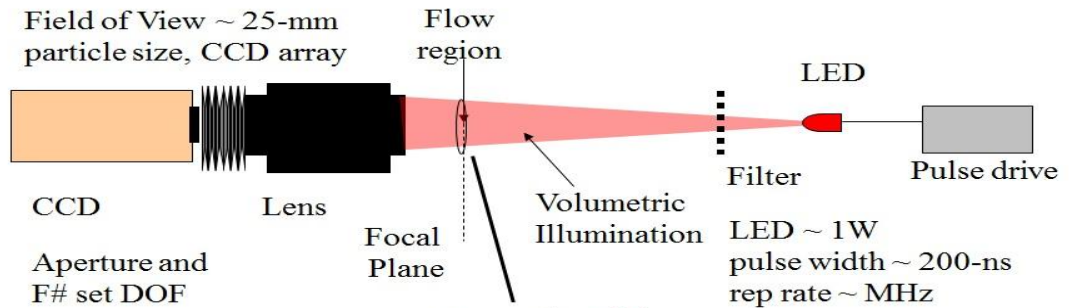
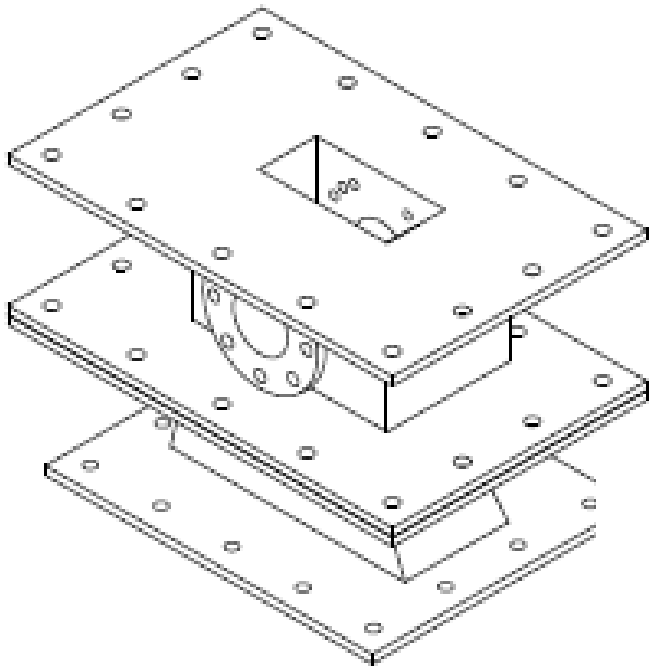
# Elastoviscoplasticity

- Technique is sensitive to the parameters desired for the deposition model
  - Temperature
  - Size
  - Mass
  - Velocity
  - Properties of the particle and surface
- Some variations include adhesion
- Calculations can easily be made for each impacting particle
  - Requires the data for yield stress
  - This data can be acquired through experimentation or empirical modeling

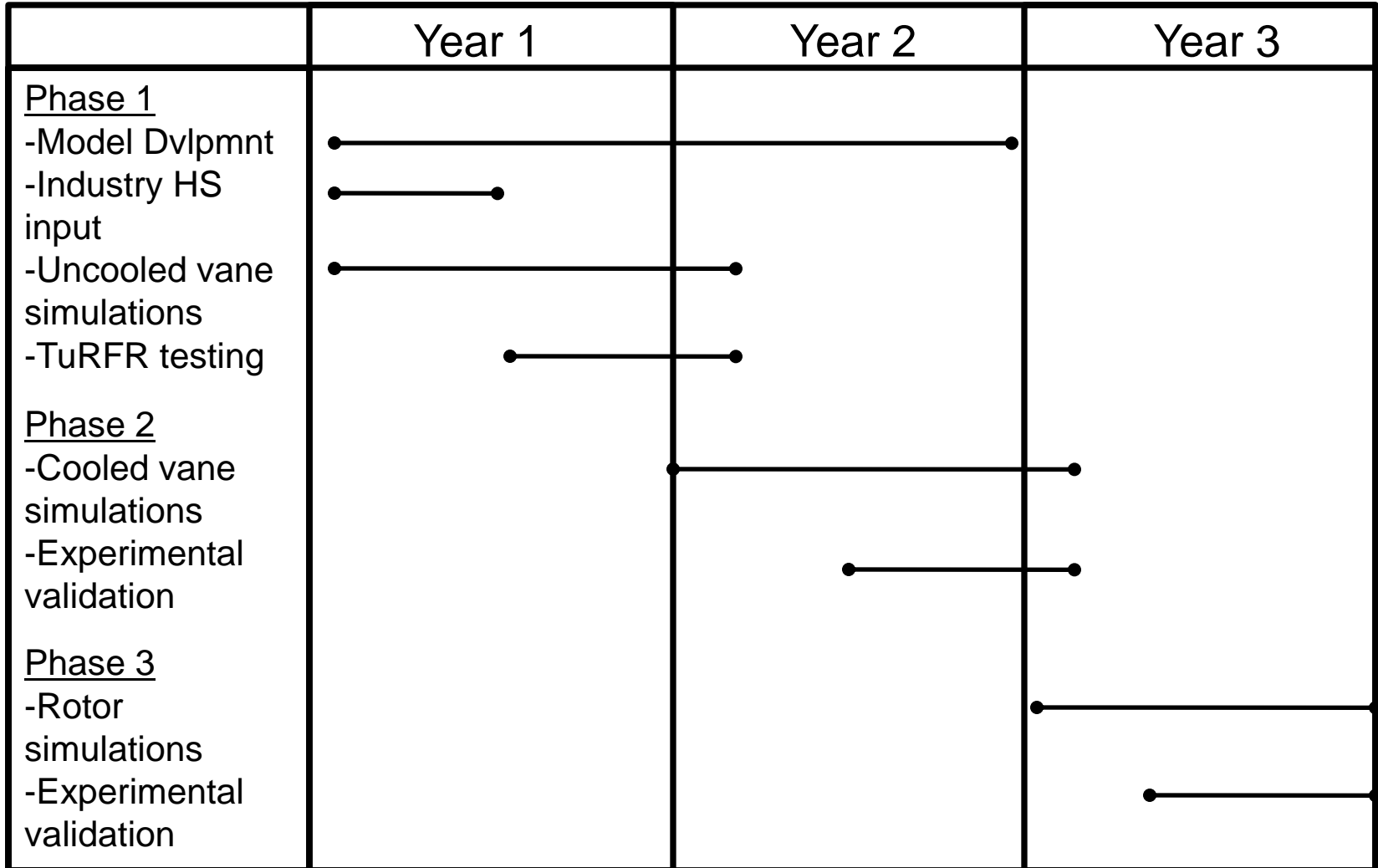


# Model Validation

- Optical test section mounted to TuRFR exit.
- Canted flat plate target.
- Particle shadow velocimetry used to measure: velocity, impact angle, sticking probability, size, acceleration



# Gantt Chart





QUESTIONS?



# Critical VELOCITY Model

## Updated

- Adjustment to rigid body model
  - Explicit parameter to represent the effect of adhesion
  - Kinetic instead of kinematic coefficient of rolling resistance
  - Modification to parameters to account for oblique impacts as well as normal impacts
  - Modification to the force term for the adhesion energy
  - Motivated by different load application points and/or distributions produce different deformations
  - Analogy to Linear Beam Theory for easier comprehension

# Critical VELOCITY Model

## Updated

- Numerical simulation model
  - Numerical integration of the equations of motion of an elastic sphere impacting on a flat plane accounting for both friction and adhesion
  - Parameters solved more systematically
  - Application to impact data showed that the weighted average approach can be used effectively and accurately to predict impact response
  - Rotational velocity can cause a variation in impulse ratio
  - Coefficient of Restitution modeled reasonably well
  - Sliding contact duration and impulse ratio value are directly related

# Critical VELOCITY Model

## Updated

- Additions
  - Rotating Particles
    - Investigated the significance of the rotational dissipation during impact
    - Material rolling deformation and peeling of the adhesion bond- proportional to the square of the radius of the particulate, can be neglected
    - Using the numerical simulation model to calculate the angular velocity of the particulate during the impact
  - Non Spherical Particles
    - Procedure is developed for stepping through the numerical simulation with non-spherical bodies
    - The results are displayed for a rod with rounded edges and two spheres connected by a rod
    - The conclusions given are that the initial orientation and initial rotational velocity of the object both have significant roles in determining the rebound characteristics of the object
  - Roughness
    - Development of a model to treat the case of static contact between a micro-particle and a flat surface in the presence of an adhesive force and surface roughness
    - Concludes that surface roughness greatly decreases the amount of force required to remove the particleDiscusses the effects of asperities on elastic and adhesive contact between smooth sphere and rough surface
      - Asperity-superposition method and direct-simulation method
    - The model predicted that the loads are not uniform and the force to remove is reduced



# Cold Spraying

- Model by Johnson and Cook
  - Calculates the Yield stress of the particle from the material properties
  - Accounts for strain, strain rate hardening and thermal softening
  - Application to finite model analysis
- Impacting metal particles at supersonic speeds
- Causes shock waves to occur in both materials
- Plastic deformation in both objects
- Penetration into the body and destruction of the particles structure

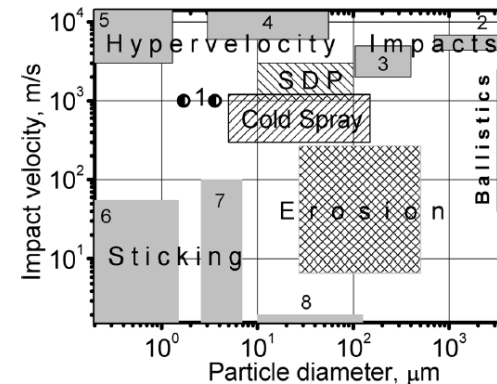


Fig. 1. Particle impact on a solid surface: Influence of impact velocity and particle size on features of the interaction. Regions characteristic of certain impact phenomena are shown. For details see text.

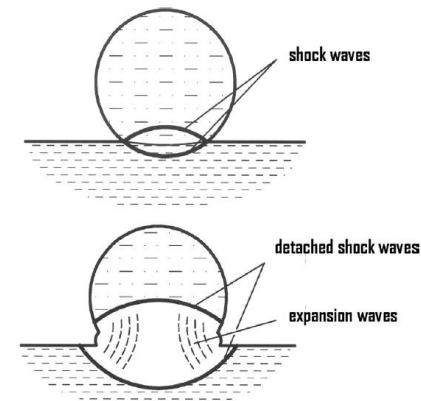


Fig. 5. Hypervelocity impacts: formation of shock and expansion waves in both the particle and the impacted body, and inception of a jetting motion (after [48]).

# Cold Spraying

- Technique is sensitive to the parameters desired for the deposition model
  - Temperature
  - Size
  - Mass
  - Velocity
  - Impingement angle
  - Properties of the particle and surface
- Technique does not include adhesion
- Technique must be solved for each individual case of particle impacting on surface
  - Available data is for high velocities
  - Many cases need to be calculated in order to form an empirical relation

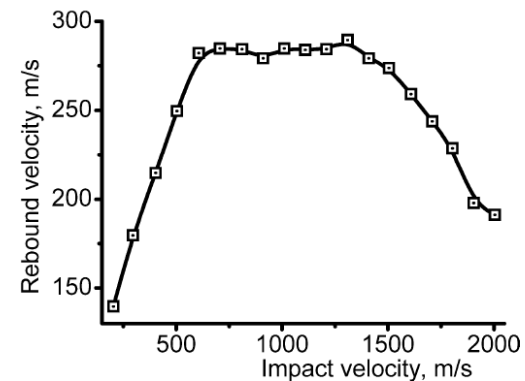


Fig. 4. Rebound velocity vs. impact velocity for spherical steel particles ( $d_p = 9.5 \mu\text{m}$ ) impinging normally onto a semi-infinite steel plate (results according to a simulation [42]).

3730

W.-Y. Li et al. / Applied Surface Science 256 (2010) 3725–3734

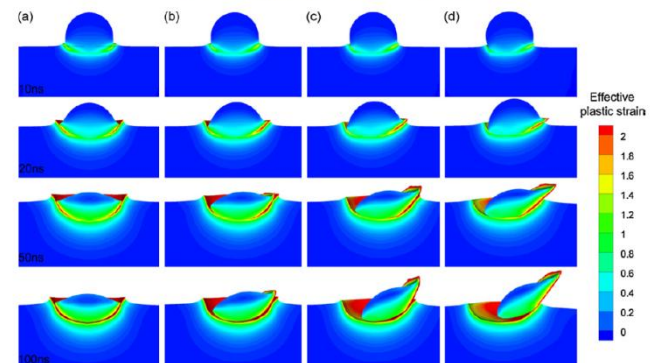


Fig. 6. Contours of the effective plastic strain as copper particles impact on copper substrates at 500 m/s with the incident angle of (a) 90°, (b) 80°, (c) 70° and (d) 60° modeled by the Lagrangian method.



# Molecular Bonding

- The Lennard-Jones Potential
  - Approximates the interaction between two neutral atoms, or molecules
  - Van der Waals attractive force, force between permanent and induced dipoles
  - Pauli repulsion force, due to the overlapping of electron orbitals at short distances
- Impacting nanoparticles on substrates
- Elastic or plastic deformation in either or both bodies
- Some of the potential between all of the atoms and the substrate

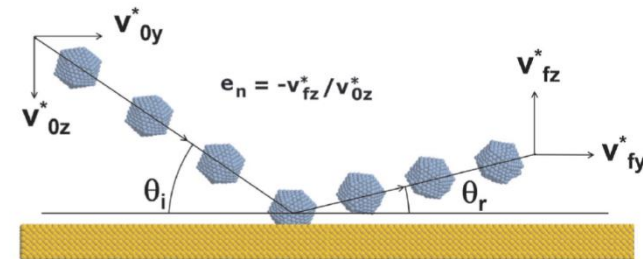


Figure 1. A series of snapshots from a simulated collision showing the definitions used for the angles of incidence,  $\theta_i$ , and reflection,  $\theta_r$ . In this case, Newton's normal coefficient of restitution is defined as  $e_n = -v_{fz}^*/v_{0z}^*$ . Newton's tangential coefficient of restitution  $e_t$  can be defined similarly as  $e_t = v_{fy}^*/v_{0y}^*$ .

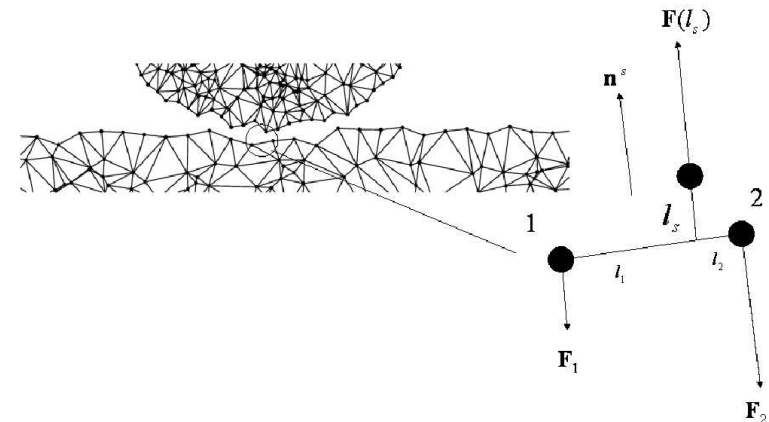


Figure 1.3: Interaction between surface particles of the disk and the wall.

# Molecular Bonding

- Technique is sensitive to the parameters desired for the deposition model
  - Temperature
  - Size
  - Mass
  - Velocity
  - Impingement Angle
  - Properties of the particle and surface
- Technique includes adhesion
- Technique must be solved for each individual case of particle impacting on surface
  - Requires detailed data on the composition and structure of both the particulate and the surface
  - Many cases need to be calculated in order to form an empirical relation

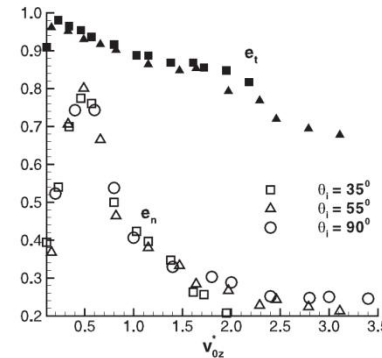


Figure 6. Newton's normal coefficient of restitution,  $e_n$  (open symbols), and tangential coefficient of restitution,  $e_t$  (closed symbols), averaged over 50 collisions with a flat surface as a function of the normal component of the incident velocity with  $C = 0.2$  at various incident angles ( $35^\circ$ ,  $55^\circ$  and  $90^\circ$ ).

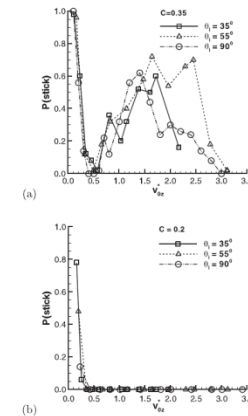


Figure 3. The probability of adhesion of the cluster incident on the flat surface, at three different incident angles ( $35^\circ$ ,  $55^\circ$  and  $90^\circ$ ), as a function of the normal component of the initial velocity,  $v_{0z}$ , averaged over 50 trials with (a)  $C = 0.35$  and (b)  $C = 0.2$ .

# FEM

- Model by Thornton Johnson and Gilibert
  - Uses the mesh of the particle and the substrate
  - Inputs require the material properties of the particle and the substrate
  - Outputs the initial and final kinetic energy of the particle
- Elastoplastic deformation of both the particle and the substrate

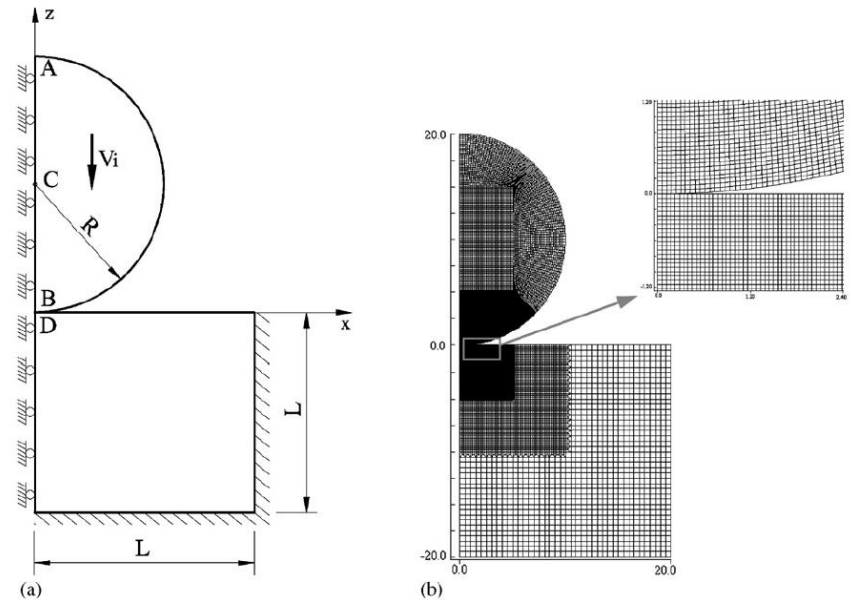


Fig. 1. Finite element model for the impact of a sphere with a half-space.

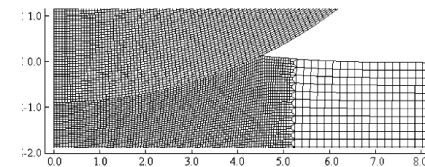


Fig. 5. Topographies of the contact deformation at the maximum compression during the impact of an elastic sphere with an elastic-perfectly plastic half-space (case 1) at  $V_i = 80$  m/s (unit:  $\mu\text{m}$ ).

# FEM

- Technique is sensitive to the parameters desired for the deposition model
  - Temperature
  - Size
  - Mass
  - Velocity
  - Impingement Angle
  - Properties of the particle and surface
- Technique includes adhesion
- Technique must be solved for each individual case of particle impacting on surface
  - Requires detailed data of the stress-strain relationship of the particulate and the substrate at varying temperature
  - This data can only be acquired through experimental data and empirical relations

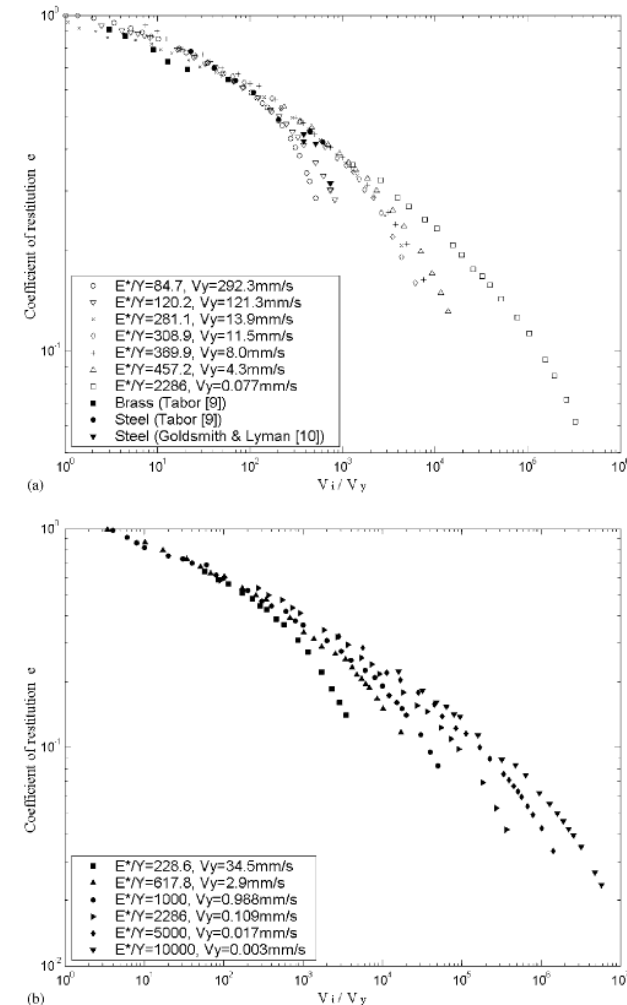


Fig. 4. Coefficient of restitution as a function of the normalized impact velocity  $V_i/V_y$  for all impact cases considered: (a) the impact of an elastic sphere with an elastic-perfectly plastic substrate, (b) the impact of an elastic-perfectly plastic sphere with a rigid wall.

# Energy Methods

- Main Model by Tsai
  - Energy stored in the elastic deformation
  - Elastic energy stored in the plastic deformation
  - Energy loss due to plastic deformation
  - Energy loss due to particles impacting on asperities
  - Sum of energy is equal to the impacting kinetic energy
- Elastoplastic particles impacting on substrate
- Elastic and/or plastic deformation in the particle

$$E_e = \frac{2}{5} \frac{a_y^5 K}{R^2}$$

$$E_{pe} = \frac{1}{2} h_y (1.1 Y) \pi a_p^2$$

$$E_p = \int_0^{a_p} P_m \pi a^2 dh,$$

$$\begin{aligned} \text{total energy} &= E_{k_1} = \frac{1}{2} m V_1^2 \\ &= E_e + E_{pe} + E_p. \end{aligned}$$

# Energy Methods

- Technique is sensitive to the parameters desired for the deposition model
  - Temperature
  - Size
  - Mass
  - Velocity
  - Electrical charging
  - Properties of the particle and surface
  - Roughness
- Technique includes adhesion
- Calculations can easily be made for each impacting particle
  - Requires detailed data of the stress-strain relationship of the particulate and the substrate at varying temperature
  - This data can only be acquired through experimental data and empirical relations

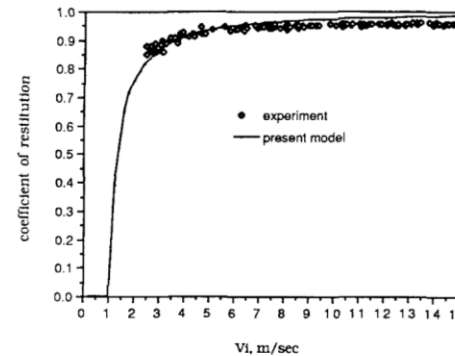
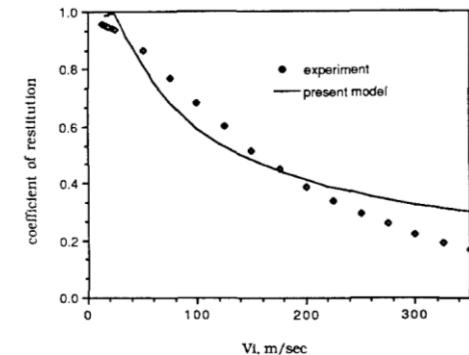


**FIGURE 6.** Comparison of the coefficient of restitution measured by Dahneke (1975) and values predicted by the present model from 0–15 m/sec.

**FIGURE 7.** Comparison of the coefficient of restitution measured by Dahneke (1975), and the values predicted by the present model from 15–350 m/sec.



# Yield Stress Determination

- Models by Green and Thornton
  - Calculates the energy stored elastically in the body
  - Determines point of plastic deformation from the Von Mises impact criteria
  - Work done by plastic deformation is calculated
  - Uses the residual interference and the Hertzian model to calculate restitution
  - Adhesion is considered in some models
- Valid only for elastic perfectly plastic particles impacting on substrate
- Elastic and/or plastic deformation in the particle

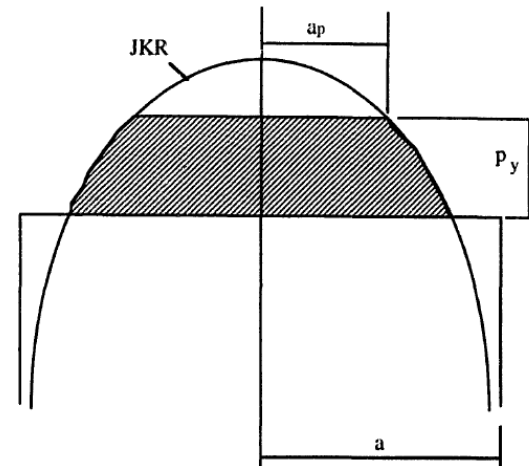
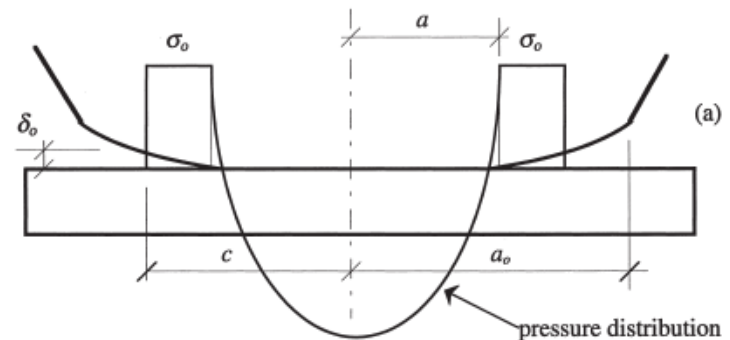


Fig. 7. Normal traction distribution for adhesive, elastic-perfectly plastic spheres.



# Yield Stress Determination

- Technique is sensitive to the parameters desired for the deposition model
  - Temperature
  - Size
  - Mass
  - Velocity
  - Oblique Impacts
  - Properties of the particle and surface
- Some variations include adhesion
- Calculations can easily be made for each impacting particle
  - Requires the data for yield stress
  - This data can be acquired through experimentation or empirical modeling

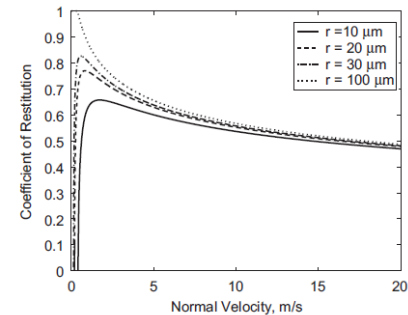


Fig. 2. The coefficient of restitution versus normal velocity for the impact of different-size aluminum-oxide microspheres with an aluminum surface.

Fig. 7 Comparison of several models to experimental results aluminum oxide spheres impacting an aluminum flat

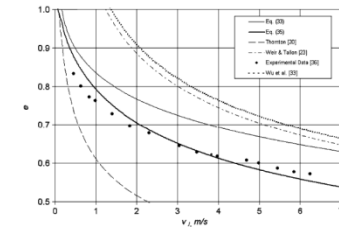
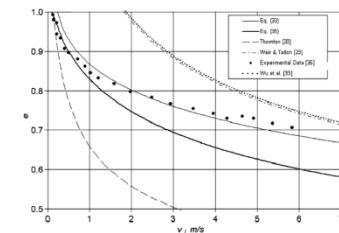


Fig. 8 Comparison of several models to experimental results aluminum oxide spheres impacting a steel flat





# Elastoviscoplasticity

- Model by Adams
  - Dependent on the mean pressure which is obtained from the flow stress corresponding to the strain rate
  - Uses the mean strain rate
  - Plastic loading
  - Herschel-Bulkley materials
  - Small amount of elastic strain
  - Does not include adhesion
- Model by Fu
  - Yield stress of impacting particle is dependent on the strain rate of the particle
  - Uses Herschel-Bulkley viscoplastic relationship to determine the modified yield stress
  - Linear elastic behavior

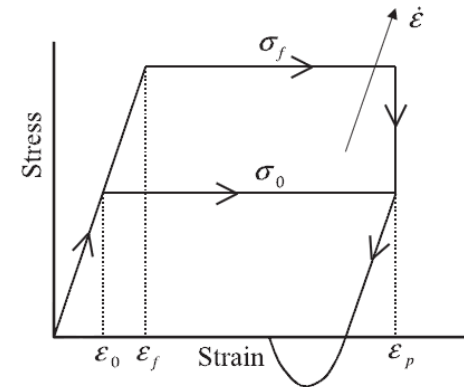
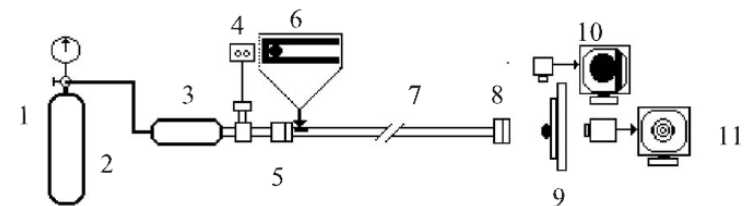


Fig. 2. Arbitrarily simple loading and unloading curves for the case that a granule is elastoviscoplastic and the impact velocity is such that the static yield stress,  $\sigma_0$ , is exceeded.



1. Air cylinder, 2. Pressure gauge, 3. Pressure cylinder, 4. Trigger, 5. Sleeve, 6. Sabot and granule, 7. Gun barrel, 8. Stopper, 9. Target, 10. High-speed camera I, 11. High-speed camera II.

Fig. 4. Schematic diagram of the compressed air gun.

# Desired Model

- Energy Methods

- Temperature
- Size
- Mass
- Velocity
- Electrical charging
- Properties of the surface
- Roughness

- Yield Stress

- Temperature
- Size
- Mass
- Velocity
- Oblique Impacts
- Properties of the surface

- Elastoviscoplasticity

- Temperature
- Size
- Mass
- Velocity
- Properties of the surface

- Energy method appears to be optimal model
  - Complexity of determining Stress vs. Strain as a  $f(T)$
- Yield stress is elastic perfectly plastic
  - Easier to implement
  - Only requires yield stress
  - Can be combined with the energy loss from roughness
- Elastoviscoplasticity model can account for stress flow and strain rates during plastic deformation

# Desired Model- The Different Pieces

- Energy Methods
  - Complicated Stress vs. Strain relationship
  - Includes Adhesion
  - Roughness
  - Electrostatic forces
  
- Elastoviscoplasticity models
  - Effects of strain rates on the yield stress
  - No Elastic Behavior
  - Incorporation of the consistency and plastic flow index

- Yield Stress
  - Elastic perfectly plastic materials
  - Thornton
    - Adhesion
    - Constant surface energy
  - Green
    - No Adhesion
    - Application of Hertzian pressure distribution



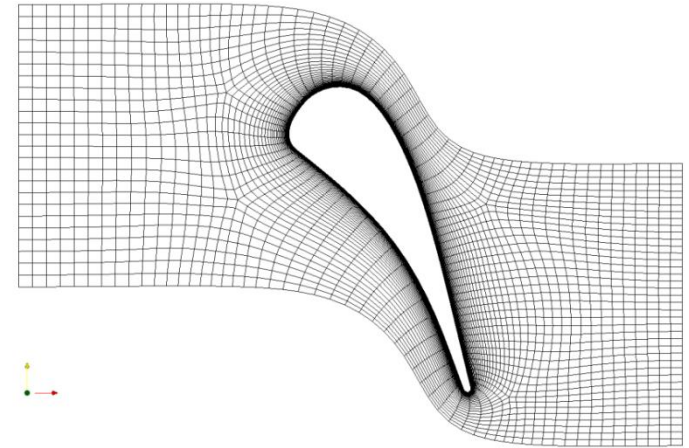
# Supplementary Slides

# Viscosity Temp. Relation

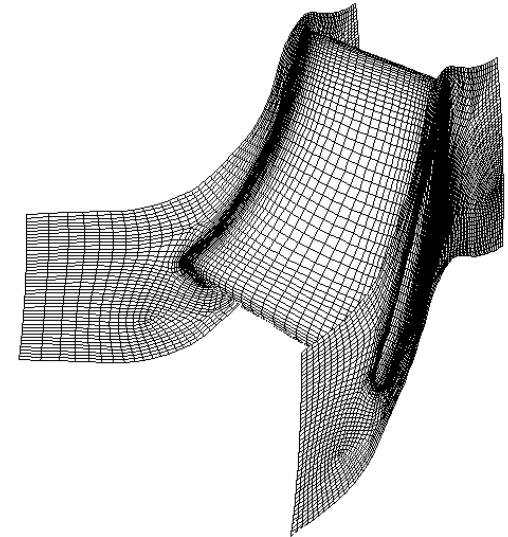
- Viscosity-Temperature relationship is necessary
- Model of Senior et. al.
  - Uses coal ash chemical composition
  - Ash is made up of a Silicate melt with a network of  $\text{SiO}_4^{4+}$
- Three categories of cations that interact with network
  - Glass formers -  $\text{Si}^{4+}$ ,  $\text{Ti}^{4+}$ , and  $\text{P}^{5+}$
  - Modifiers -  $\text{Ca}^{2+}$ ,  $\text{Mg}^{2+}$ ,  $\text{Fe}^{2+}$ ,  $\text{K}^+$  and  $\text{Na}^+$
  - Amphoteric -  $\text{Al}^{3+}$ ,  $\text{Fe}^{3+}$ , and  $\text{B}^{3+}$

# Flow Physics

- Flow solution using FLUENT
  - Commercially available
  - Solves discretized flow equations to predict fluid dynamics
- Deposition Models
  - developed in C language and incorporated as User-Defined Functions in Fluent
- Turbine grid made using GridPro
  - VKI Turbine Vane
  - GE-E<sup>3</sup> Turbine Vane



VKI Turbine Vane (2D)



E<sup>3</sup> Turbine Vane (3D)